Filament Organization Revealed in Platinum Replicas of Freeze-dried Cytoskeletons

J. E. HEUSER, and M. W. KIRSCHNER

*Departments of Physiology, Biochemistry, and Biophysics, School of Medicine, University of California, San Francisco, California 94143, *Current address: Dept. of Physiology and Biophysics, Washington Univ., School of Medicine, St. Louis, MO 63110*

ABSTRACT This report presents the appearance of rapidly frozen, freeze-dried cytoskeletons that have been rotary replicated with platinum and viewed in the transmission electron microscope. The resolution of this method is sufficient to visualize individual filaments in the cytoskeleton and to discriminate among actin, microtubules, and intermediate filaments solely by their surface substructure. This identification has been confirmed by specific decoration with antibodies and selective extraction of individual filament types, and correlated with light microscope immunocytochemistry and gel electrophoresis patterns.

The freeze-drying preserves a remarkable degree of three-dimensionality in the organization of these cytoskeletons. They look strikingly similar to the meshwork of strands or "microtrabeculae" seen in the cytoplasm of whole cells by high voltage electron microscopy, in that the filaments form a lattice of the same configuration and with the same proportions of open area as the microtrabeculae seen in whole cells. The major differences between these two views of the structural elements of the cytoplasmic matrix can be attributed to the effects of aldehyde fixation and dehydration.

Freeze-dried cytoskeletons thus provide an opportunity to study—at high resolution and in the absence of problems caused by chemical fixation—the detailed organization of filaments in different regions of the cytoplasm and at different stages of cell development. In this report the pattern of actin and intermediate filament organization in various regions of fully spread mouse fibroblasts is described.

In recent years more and more attention has been directed toward the role of intracellular filamentous proteins in the determination of cell morphology and in the direction of cell movement. An important technical advance in isolating and visualizing these filaments has come from the discovery that extraction of living cells with nonionic detergents leaves behind a residuum that contains a large proportion of the cellular actin and intermediate filament protein (4, 20, 21). The cell's microtubules may also be preserved in this residuum under specific stabilizing conditions (3, 7, 22). This framework of filaments, which remains after detergent extraction, has been termed the cytoskeleton.

Light microscope immunocytochemistry has illustrated that the cytoskeleton contains many of the components thought to be involved in cell motility, in arrangements similar to that found in unextracted cells. For example, Osborn and Weber (21, 22) and Webster et al. (29) have demonstrated close similarities in the filament distributions in cytoskeletons vs. whole cells, by immunofluorescence, using antibodies to actin, myosin, tropomyosin, α-actinin, tonofilaments, and tubulin. All of these antibodies bind avidly to cytoskeletons, and in fact some, including those directed against microtubules, bind to extracted cells with better definition and lower backgrounds than they do to intact cells (22, 27). These results vividly demonstrate that the cytoskeleton can serve as an excellent representation of the filaments in intact cells, at least at the level of resolution of the light microscope.

Attempts to determine how filaments in the cytoskeleton are organized on an ultrastructural level have been limited primarily by the methods used to prepare them as whole mounts for electron microscopy. In a recent protocol of Bell et al. (2) cells were cross-linked with a diimidoester, extracted with Triton X-100 (Triton) and then fixed by the standard aldehyde and osmium sequence, followed by dehydration, critical-point drying, and viewing in the scanning electron microscope. Critical-point drying prevented the collapse of the filaments and

THE JOURNAL OF CELL BIOLOGY · VOLUME 86 JULY 1980 212-234

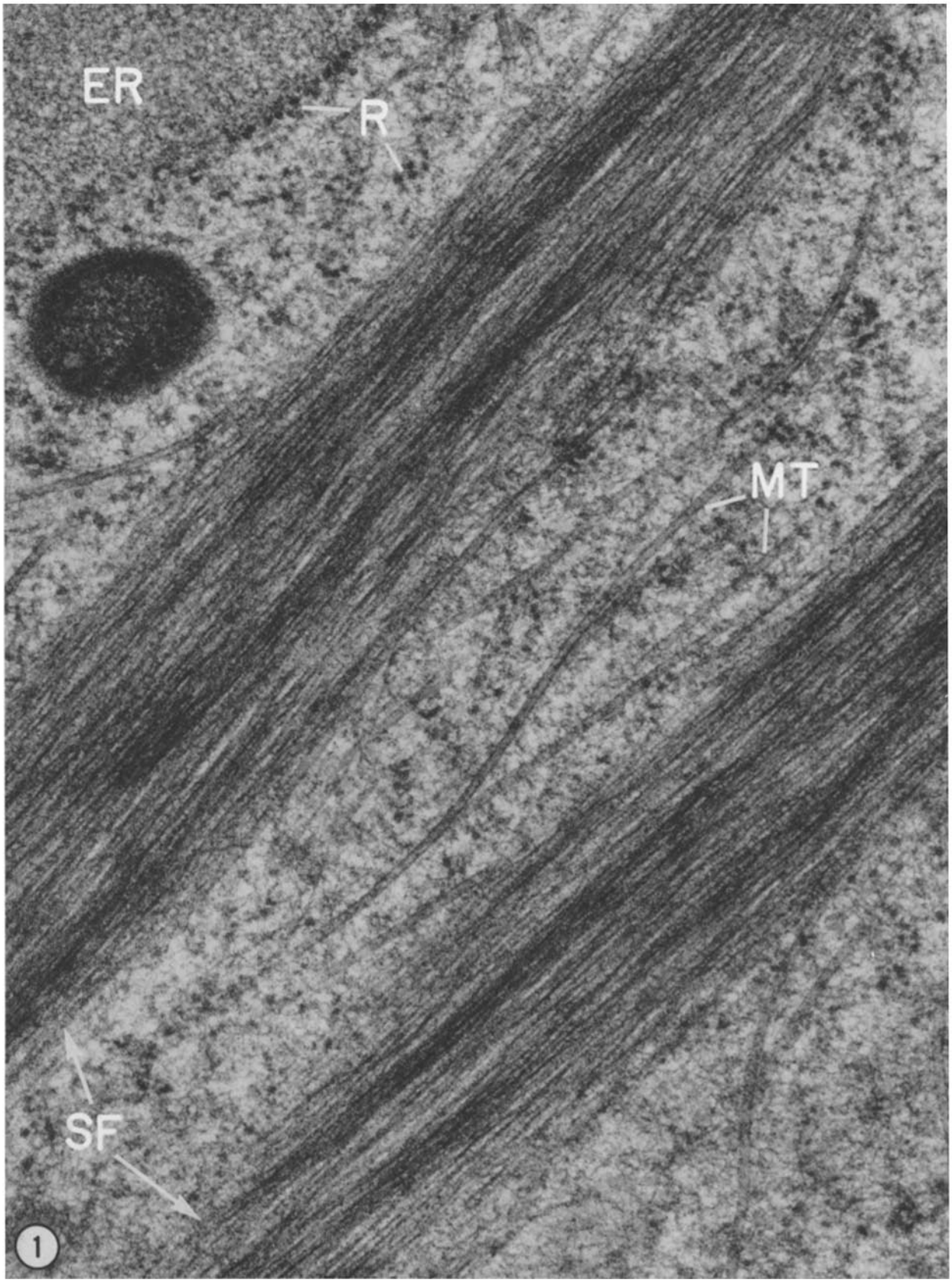

FIGURE 1 Traditional thin section of a fibroblast that was quick-frozen with a liquid helium-cooled block of copper, and then freeze-substituted in acetone-osmium at −90°C for 2 d, to illustrate the overall quality of freezing that could be achieved. Ice crystals are too small to disturb the close packing of filaments in the stress fibers (*SF*), and too small to disturb the random distribution of protein inside the cisternae of the endoplasmic reticulum (*ER*); the only hint of their presence is the small lucent area around the mitochondrion. Ribosomes (*R*) and microtubules (*MT*) look well preserved, and lie in a background matrix that looks delicately floccular. × 85,000.

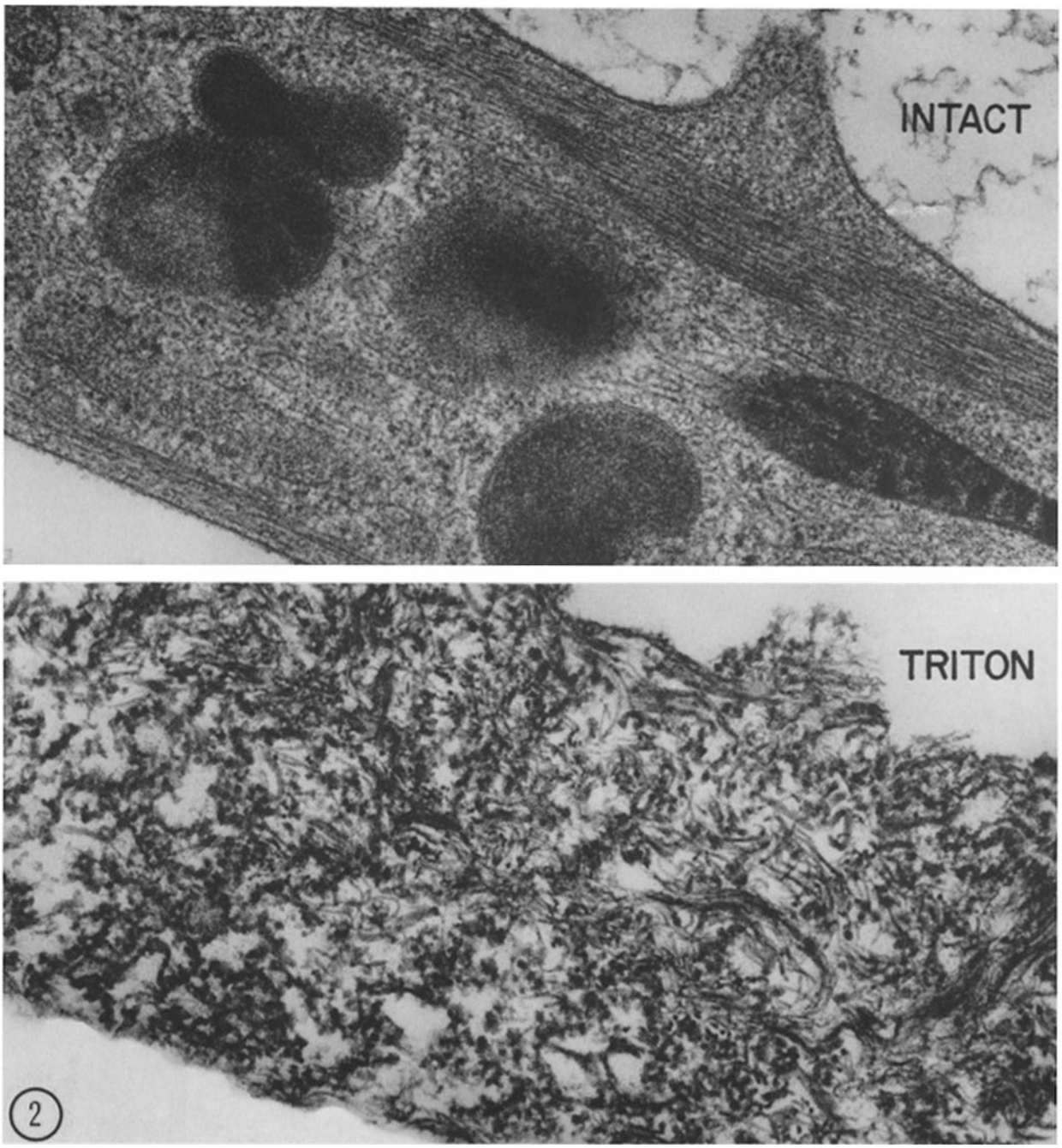

FIGURE 2 Cross section through an intact fibroblast prepared as in Fig. 1 (*INTACT*) compared with a section through a cytoskeleton prepared by exposing a living cell to 0.5% Triton for 30 min (*TRITON*). Membranous organelles and surface membranes are gone from the skeleton, but a rich complement of filaments is left behind. (Here the electron density of these filaments was accentuated by block-staining in 0.2% hafnium chloride in acetone for 1 h after freeze-substitution.) The pattern of filament organization cannot be easily discerned in such 0.1-μm-thick sections, but is more easily assessed in the platinum surface replicas that follow. × 70,000.

provided some sense of their three-dimensional organization. However, the filaments appeared variable in thickness as a result of the gold shadowing, and the resolution of the scanning electron microscope was not good enough to image the interactions of filaments with each other, or to identify structurally the various filament types. Nevertheless, this approach illustrated that the cytoskeletons are somewhat thinner than the whole cells, and comprise primarily the lower portions of the cells, the regions where most stress fibers occur. In many instances, the cell nucleus remains attached to this cytoplasmic foundation, but little appears to remain of the protoplasmic components that lie immediately under the plasma membrane or in the region above the nucleus.

Efforts were made originally to view cytoskeletons at high resolution employing uranyl acetate staining after aldehyde fixation, followed by air-drying. As shown by Brown et al. (4) and Small and Celis (26), air-drying causes collapse of the cytoskeletons. However, they could then be viewed flat in the transmission electron microscope at sufficient resolution to demonstrate that stress fibers and other major struts in the

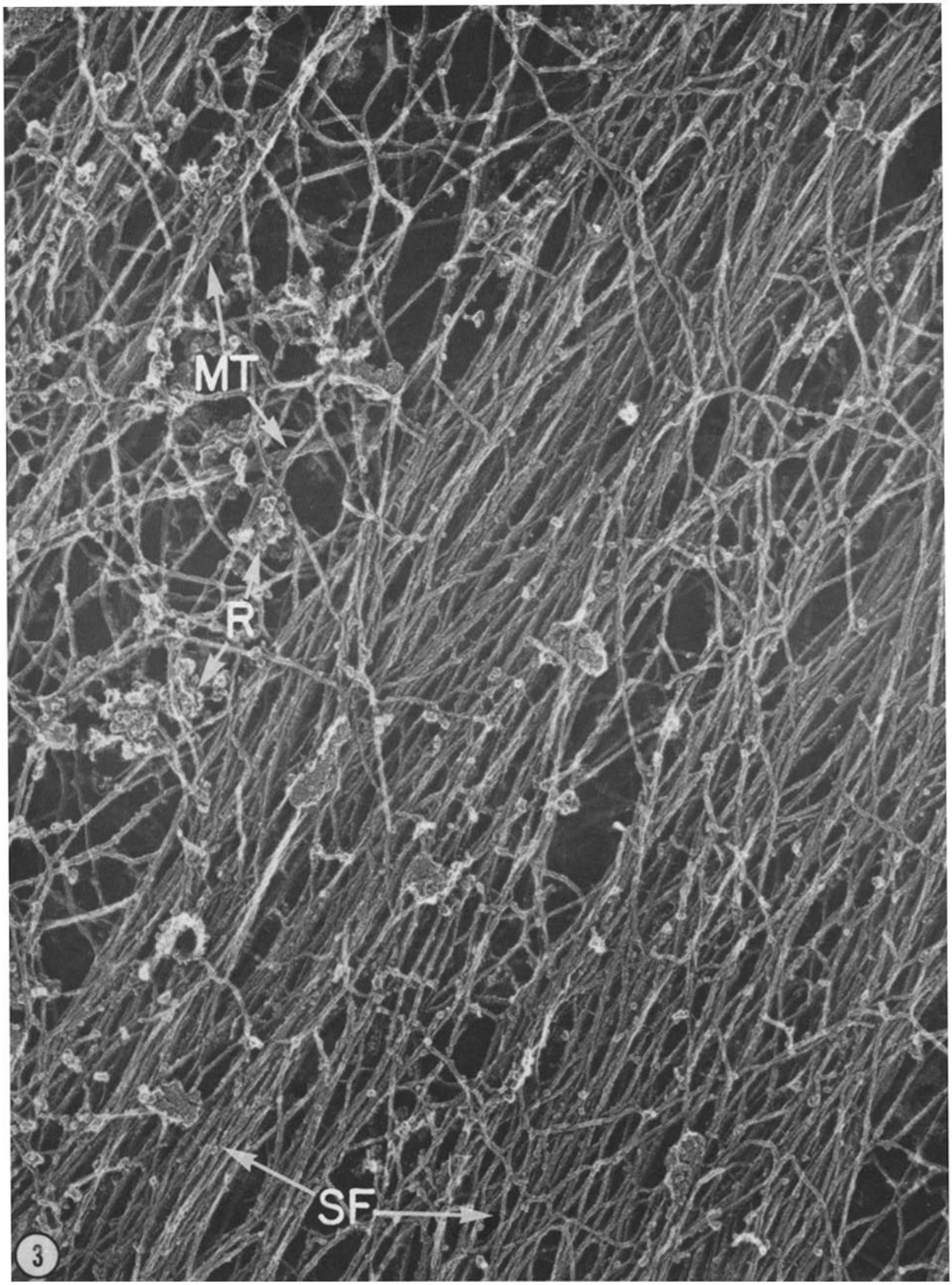

FIGURE 3 Rotary-deposited platinum replica of a freeze-dried cytoskeleton, from a fibroblast that was extracted for 30 min with 0.5% Triton. Prominent are the bundles of filaments that comprise what must have been the cells' stress fibers (*SF*). Also visible in the upper left-hand corner are two thicker structures thought to be microtubules (*MT*), and a more diffuse meshwork of filaments that is studded here and there with grapelike clusters that are the size and shape of polyribosomes (*R*). (Note: Figs. 2, 3, 7, 10, 12, 16, and 17 are all printed in the same × 70,000 magnification to facilitate comparison of the results of different experiments described herein.)

cytoskeleton are composed of bundles of 60–70 Å and 100 Å filaments. This was consistent with the biochemical and immunocytochemical analyses of the cytoskeletons, which illustrated that they contain primarily actin and intermediate filament protein (2, 4, 20, 21, 29).

More recently, Webster et al. (28) have amalgamated these preparative methods by critical-point drying cytoskeletons after aldehyde fixation and uranyl acetate staining, thus producing specimens that are beautifully three-dimensional and highly informative when viewed by stereo transmission electron microscopy. By this method, the most prevalent component of the cytoskeleton is a branched, anastomotic network, which decorates with ferritin labeled anti-actin antibodies.

A totally different approach to visualizing the polymeric elements of cytoplasm, which does not rely upon selective extraction and preparation of cytoskeletons, has been introduced by Porter and co-workers. They examined whole cells, grown on electron microscope grids, that they fixed with aldehyde and osmium tetroxide and then critical-point dried before viewing first with the standard transmission electron microscope and later with the high voltage electron microscope (5, 31, 32). In these preparations, whole cells exhibit a fine anastomotic three-dimensional network, composed of what Wolosowick and Porter call "microtrabeculae." This network looks so similar to the ones seen by Webster et al. (28) in cytoskeletons after critical-point drying, that it is tempting to conclude they are identical. However, that conclusion would imply that actin is the most prevalent component of the microtrabeculae. Yet, the microtrabeculae seen in whole cells are much more variable in shape and diameter than any known form of actin polymer. Wolosowick and Porter (32) report that they vary from <30 Å to >100 Å in diameter, whereas actin is known to polymerize into filaments of uniform diameter of ~60 Å. Moreover, microtrabeculae appear to branch or anastomose with each other at smooth, continuous junctions that do not look like simple points of filament crossover.

To determine how the images of whole cells relate to the filamentous cytoskeletons prepared by detergent extraction, we have examined both whole and Triton-extracted cells after preparing them for electron microscopy by quick-freezing at liquid helium temperature. The freezing method avoids the problems of chemical fixation and dehydration. Cytoskeletons of fibroblast cells viewed by this new protocol of extraction, rapid freezing, freeze-drying, and rotary shadowing offer new and informative images of the actin, intermediate filament, and microtubule arrays in different regions of the cell under different physiological conditions. The method has sufficient resolution to identify different filament types by their structure alone. When we compared these new images with those obtained after cells were pretreated with aldehydes, it appeared that the microtrabeculae may actually be composed of discrete filamentous components of the cytoskeleton that seem to have become cross-linked, thickened, and partly obscured by adsorption of soluble cytoplasmic proteins during the process of chemical fixation.

MATERIALS AND METHODS

Cell Culture

Fibroblast cells were isolated by trypsinization from BALB/c mouse embryos and used within four passages. They were plated onto 60-mm Falcon tissue culture dishes (Falcon Labware, Div. Becton, Dickinson & Co., Oxnard, Calif.) containing a number of 4-mm-square fragments of no. 1 Corning cover glass (Corning Glass Works, Scientific Products Div., Corning, N. Y.) and maintained in Dulbecco's Modified Eagle's Minimal Essential Medium with 10% fetal calf serum. Cells were allowed to attach and spread on the glass coverslips for 18 h before each experiment.

Preparation of Cytoskeletons

Cytoskeletons containing actin, intermediate filaments, and microtubules were prepared in the following manner: Each dish of cells containing several glass coverslip fragments was washed for 1 min in phosphate-buffered saline at 37°C, followed by 1 min at 37°C in a buffer commonly used to polymerize and stabilize microtubules, which we will refer to as "stabilization buffer," (0.1 M PIPES at pH 6.9, 0.5 mM $MgCl_2$, 0.1 mM EDTA), followed by stabilization buffer plus 0.5% Triton and 4 M glycerol at 37°C. The glycerol was added simultaneously to the Triton to further stabilize microtubules as the Triton dissolved away the plasma membrane. (cf., reference 3). After 3 min an equal volume of stabilization buffer plus 4 M glycerol and 4% glutaraldehyde was added with very gentle mixing to give a final glutaraldehyde concentration of 2%. This was allowed to remain at 22°C for 30 min before washing with five changes in distilled water.

Cytoskeletons containing actin but no microtubules were prepared as above except that the glycerol was omitted during the Triton extraction. The extraction was allowed to proceed for 30–60 min, after which the cytoskeletons were washed with stabilization buffer. They were then fixed with 2% glutaraldehyde in stabilization buffer for 30 min and washed five times with distilled water. For subfragment 1 (S1) decoration of actin-containing cytoskeletons, S1 at a concentration of 3 mg/ml in stabilization buffer (provided by Dr. Roger Cooke and prepared according to the procedure of Cooke (9), was added to the cytoskeletons before the fixation step. After 10 min, the coverslips were rinsed twice with stabilization buffer and then fixed with 2% glutaraldehyde and washed with distilled water.

Actin was extracted from cytoskeletons by the following procedure. Cytoskeletons prepared in the absence of glycerol were incubated with 0.3 M potassium iodide (KI) for 3 h at 4°C. The coverslips were then washed with stabilization buffer and fixed for 30 min in stabilization buffer plus 2% glutaraldehyde.

Immunofluorescence of the Cytoskeletons

Cytoskeletons prepared by the protocols listed above were stained with antibodies, using indirect immunofluorescence. Before the glutaraldehyde fixation step, the coverslips were plunged into methanol at 20°C, washed in saline, treated with primary rabbit antiserum against tubulin, followed by reaction with fluorescein-conjugated goat anti-rabbit antibody as described previously (27). Antibody to tubulin was prepared from putrified chick brain tubulin by the procedure of Connolly et al. (8). Antibody to the hamster 58,000-dalton protein (intermediate filament protein) was a kind gift of Dr. Richard Hynes (Massachusetts Institute of Technology, Cambridge, Mass.) (16). Antibody to actin was the kind gift of Dr. Robert Pollack (Columbia University, New York) and Dr. Keith Burridge (Cold Spring Harbor Laboratory, Cold Spring Harbor, N. Y.) (6).

Preparation of Microtubules

Microtubules from chicken brain were purified by three cycles of polymerization-depolymerization according to the Weingarten et al. (30) modification of the Shelanski et al. (25) procedure. They were resuspended in stabilization buffer at 37°C at a concentration of 8 mg/ml and quick frozen, fractured, and deep etched.

Quick Freezing of Samples

After washing in distilled water, the coverslips were rinsed in 10% methanol in water. We found that 10% methanol acts as a very good cryoprotectant; that is, it reduces the size of the ice crystals formed at a given rate of freezing, and yet it is volatile at the temperatures used for freeze-drying. It has no observable effect on the structures of purified actin and microtubules, nor on the overall appearance of the cytoskeleton.

Freezing was performed by mounting the cover glass on a 1-cm-diameter aluminum disk at the end of a plunger device, originally designed to catch exocytosis in isolated frog muscles. The plunger slams the sample down against a pure copper block cooled to liquid helium temperatures (13). This produced frozen cytoskeletons embedded in microcrystalline ice. The ice crystal size was smaller than 50 nm as a result of the extremely rapid freezing and the help of the volatile cryoprotectant (methanol). To avoid crushing the cytoskeleton and shattering the cover glass when the holder made forceful contact with the cold copper block, the cover glasses were mounted on a soft, spongy matrix composed of slices of aldehyde-fixed rat lung. The lungs had been cut 0.8 mm thick with a Smith-Farquhar tissue chopper and washed for weeks in distilled water before use. As they froze, the slices of lung became bonded to the surface of the

aluminum disk. The disks could then be mounted on the standard rotary specimen stage of the Balzers freeze-fracture device (Balzers Corp., Hudson, N. H.).

Freeze-drying and Replication

The frozen cytoskeletons on cover glasses were kept covered with a small aluminum cap as they were transferred and clamped into the vacuum evaporator. Once a vacuum of 10^{-4} torr was achieved, the cap was removed with a special vacuum feed-through. Then the samples were warmed to −95°C at a vacuum of 10^{-6} torr or better for 30–60 min, in order to sublime away all the ice from the top of the cover glass. Because there were no solutes or nonvolatile cryoprotectants in this ice, there was no scum left behind after freeze-drying. As discussed in Results, the exposed cytoskeletons did not appear to collapse very much at −95°C, though we found they could collapse and become distorted if warmed much above −80°C.

After this procedure, the freeze-dried skeletons could be viewed directly in the electron microscope, if the cells had been originally grown on Formvar-coated gold microscope grids instead of on glass. Alternatively, they could be stained with osmium vapor at ambient temperature and pressure before viewing. In either case we found that the cytoskeletons warmed and melted considerably in the 100-kV electron beam. Freeze-dried skeletons on glass were best viewed after coating with a thin layer of platinum-carbon applied in the rotary mode. In this procedure, the sample, after freeze-drying and still at −95°C, was exposed to evaporation of platinum-carbon from an electron beam gun mounted at 24° to the specimen plane, while the specimen was rotating at 60 rpm. The resulting platinum "replica" of the cytoskeleton was stabilized by 5 s of rotary deposition of pure carbon from a gun mounted at 75° to the sample plane. The sample and the cover glass were then removed from the vacuum evaporator and the cover glass floated off the adhering lung by placing it in 30% hydrofluoric acid, which also promptly released the replica from its surface. The replica was then floated sequentially through distilled water, household bleach, and two washes of distilled water before being picked up on a 75-mesh formvar-carbon-coated copper grid.

Examination was carried out in a JEOL 100B or 100C electron microscope operating at 100 kV. The high accelerating voltage was used to reduce heating of the replica, to minimize recrystallization, and also to reduce contrast in the final photographic negative. Stereo pairs were obtained with a high-resolution top-entry goniometer, stage tilted through ±6° for all magnifications. Micrographs were examined in negative contrast, i.e., by projecting the original electron microscopic negatives or by photographically reversing them before printing, to make platinum deposits look white and background look dark. The reversed contrast enhanced the three-dimensional appearance of the images, and made the skeletons look as if they were illuminated by diffuse "moonlight" very much the way samples look in the standard mode of scanning electron microscopy.

RESULTS

Assessment of Cell Structure after Rapid Freezing

Because the quality of structural preservation of the filament network could be no better than the initial quality of freezing, this was first evaluated by freeze-substituting whole cells that had been grown on cover glasses and rapidly frozen while alive, without prior Triton extraction. Freeze-substitution was by standard techniques. Cells thin-sectioned parallel to the culture dish (Fig. 1) displayed membranous organelles and filamentous actin bundles and microtubules typical of fibroblasts, in a natural-looking state of preservation. The background cytoplasmic matrix looked uniformly dense at lower magnifications and slightly lacy or flocculent at higher magnifications.

The effects of Triton on such tissue culture cells could be evaluated by cross-sectioning them after freeze substitution. Unextracted cells displayed the usual complement of membranous organelles and cytoplasmic filaments embedded in a vaguely wispy cytoplasmic matrix (Fig. 2 *a*). Freezing was often good all the way down to the surface of the cover glass on which the cells were grown. In contrast, cells extracted with Triton for 3 min or longer had lost their plasma membrane and most of their internal membranous organelles. Left behind were rich tangles of filaments, whose prominence could be enhanced after freeze-substitution by block staining with tannic acid or with hafnium chloride (as was done in Fig. 2 *b*), but whose pattern of organization could not easily be discerned in routine thin sections.[1]

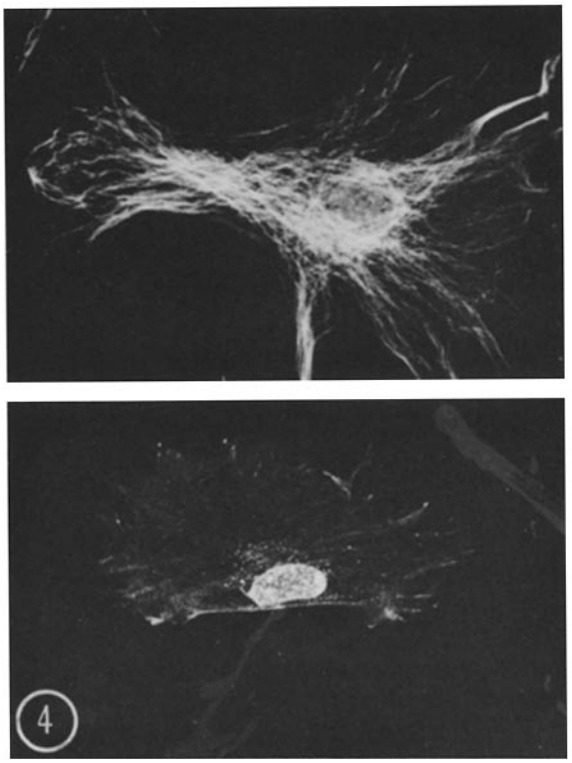

FIGURE 4 Antitubulin immunofluorescence of a mouse fibroblast cytoskeleton prepared by Triton extraction in glycerol stabilization medium (top) vs. a fibroblast cytoskeleton extracted in the absence of glycerol (bottom), which results in the loss of microtubules. × 1,000.

Assessment of Freeze-drying

Rotary replicas of freeze-dried cytoskeletons displayed a high degree of structural preservation and detail (Fig. 3). The extracted cells appeared to be composed of myriads of long filaments that overlapped and intersected each other in complex patterns. The most obvious pattern was parallel alignment of many dozens of filaments into broad bundles that presumably represented the stress fibers seen in light microscopy. Other patterns appeared to be more isotropic in three dimensions, and thus represented webs woven out of individual filaments or small groups of filaments that crossed and inter-

[1] Block-staining with hafnium chloride (M. Karnovsky, personal communication) or tannic acid was employed after freeze-substitution. If either treatment was allowed to continue too long, it increased the electron density of the cytoplasmic matrix of whole cells to such a great extent that it became impossible to discern individual filamentous components. Instead, the cytoplasm of whole cells appeared to be a dense lacy spongework surrounding translucent holes, which varied from <200 Å in the best-frozen areas to >1,000 Å in the areas where membranous organelles began to look "cobblestoned" and otherwise badly frozen. Presumably, these holes represented pure ice crystals that had formed during freezing and had pushed aside the stainable components of the cytoplasm. Similar ice crystals must have formed in the cytoskeletons, but they must have been small enough not to leave permanent distortions after freeze-drying.

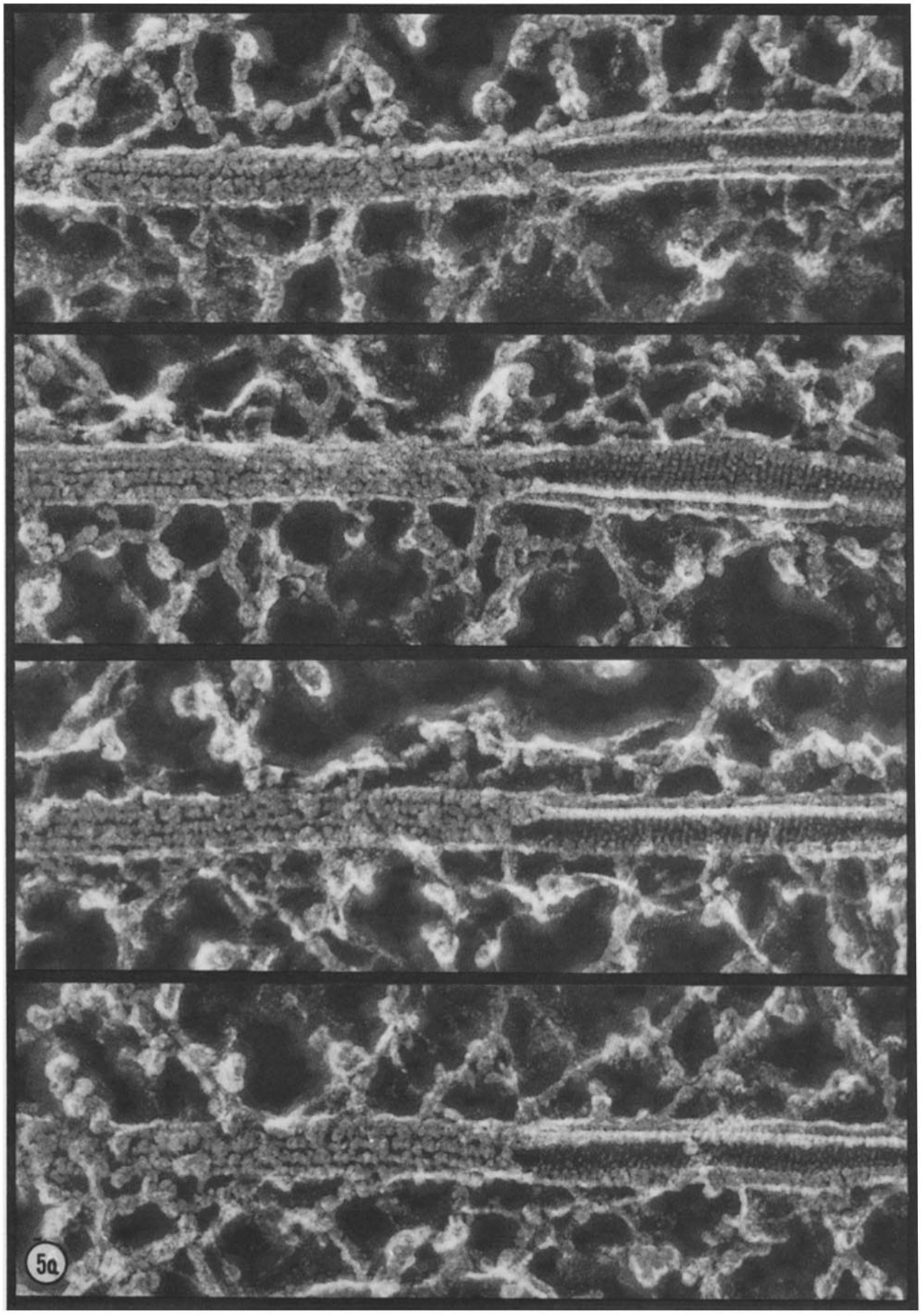
5a

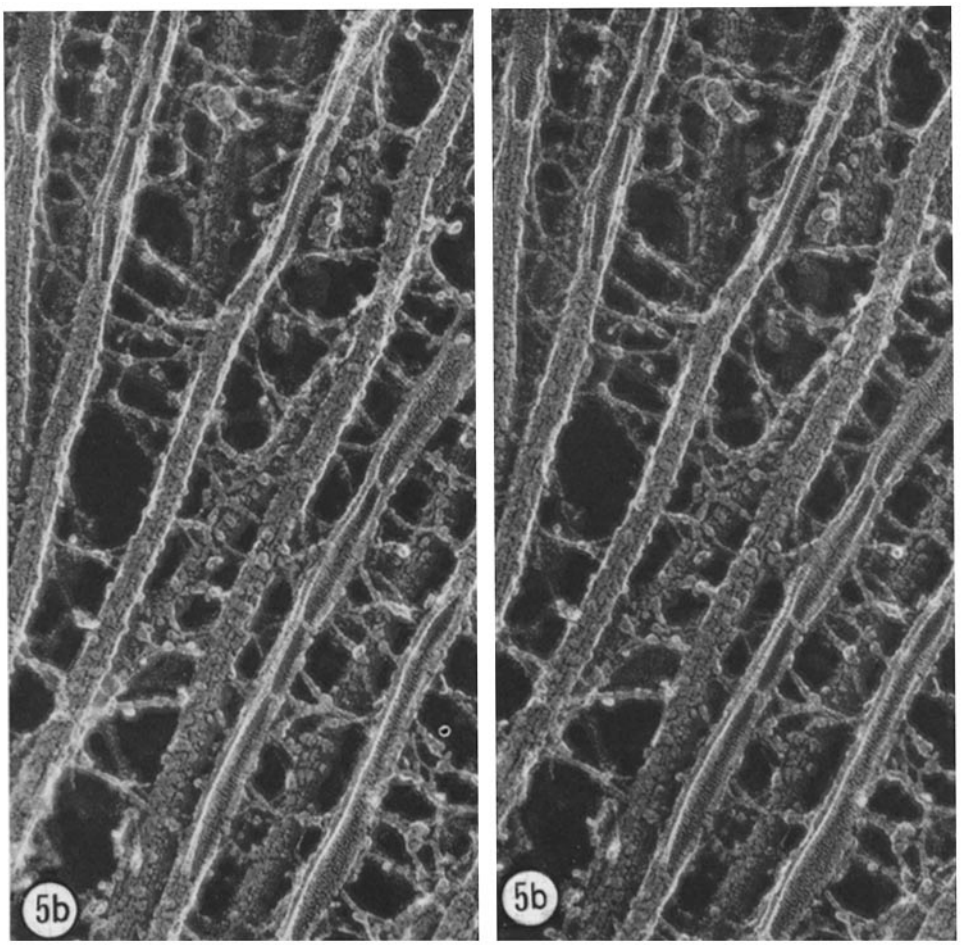

FIGURE 5 High magnification of purified microtubules that were fractured and deep etched after quick-freezing, to illustrate the resolution of the rotary replication technique. In the four examples shown in *a*, the left half of the field illustrates the outer surface of the microtubules, which display longitudinal bands of bumps spaced 55 Å apart, which may represent the microtubule's protofilaments. To the right of each figure, the microtubules are fractured open to reveal their inner luminal walls, which display characteristic oblique striations separated by 40 Å. This 3-start helix has been seen before only in optically filtered electron micrographs. (The reticulum surrounding the microtubules is thought to be unpolymerized tubulin and microtubule-associated proteins. In *b*, a similar field is shown in stereo, to illustrate more clearly the three-dimensional organization of the inner and outer substructure visible in freeze-dried microtubules. *a*, × 350,000; *b*, × 200,000.

digitated. These webs could be found between the stress fibers and above stress fibers in the areas that may have contained the organelle-rich "endoplasm" of the fibroblasts before detergent extraction.

At the magnifications that showed up the individual filaments in these skeletons, microtubules were relatively sparse and ran a relatively straight course right through the middle of the filament webs, though they did not appear to penetrate the more compact bundles of filaments. Lateral contacts between microtubules and other filaments were common, but there was no visual cue to specificity or order in this association. (Much may have been missed here, however, because these microtubules had been pre-fixed with glutaraldehyde before freeze-drying. The problem we faced was that unfixed microtubules had to be maintained in glycerol at a salt concentration of >25 mM or they would depolymerize [cf. Fig. 4], but that much nonvolatile material left behind an impossible scum when the cytoskeletons were totally freeze-dried. Only after the main body of work in this paper was done did the agent Taxol, which aided in stabilizing microtubules at low ionic strength [24], become available.)

Stereo views of the substructure of purified microtubules such as those seen in Fig. 5 illustrated the resolution of the rotary replicas. Purified microtubules were pelleted in 100 mM salt and then quick-frozen without fixation. The salt made it impossible to freeze-dry the entire pellet, but a portion could be exposed by deep-etching it for 3 min after freeze-fracture. The outside surface of these microtubules demonstrated several parallel arrays of bumps having a periodicity of ~40 Å. These arrays undoubtedly represented the subunits in the 13 protofilaments of the microtubule. Also visible in regions where a microtubule had been broken open by the fracture was a substructure on its inner surface, against its lumen. There, the subunits accentuated the 3-start helix, which had previously only been detected by optical filtering of negative stain electron microscopic images (1, 10, 12). Though the resolution of these platinum replicas was not as high as with negative stain, it could easily pick up the 40-Å repeat, and offered the advantage that inner and outer surfaces could be visualized independently. We will show next that the resolution of the technique was sufficient to distinguish differences among the various filament types in the intact cytoskeleton.

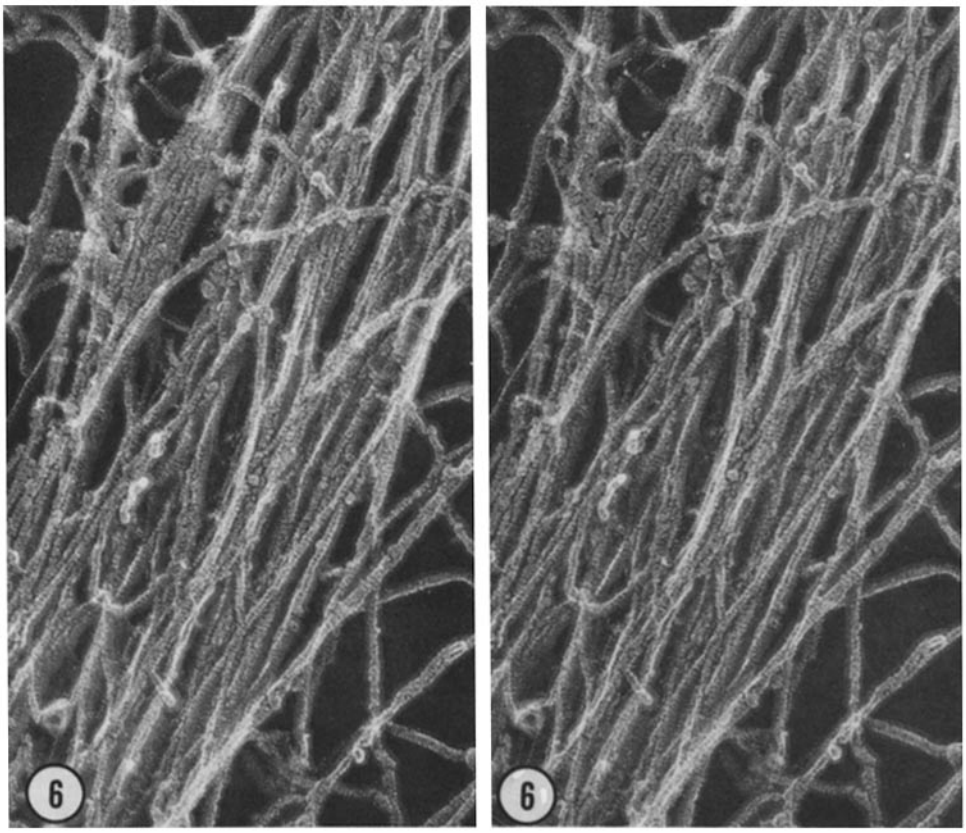

FIGURE 6 Stereo views of the bundles of filaments found in fully spread fibroblasts, which allow the observer to discern the individual filaments more clearly, to appreciate the characteristic granularity of their coat of platinum, and to discern how they are bundled together. These features are harder to see on flat views such as Fig. 3. × 200,000.

Identification of Filament Types in the Cytoskeleton

High magnification stereo views of the bundles of filaments that made up what may have been stress fibers in the whole cells, as shown in Fig. 6, allowed ready discrimination of the individual filaments. These filaments appeared to have a relatively uniform caliber of 95 ± 10 Å along their entire length. Typically, the replicas of these filaments displayed a coarse, vaguely striped pattern of platinum granularity, spaced about every 50–60 Å. Such a pattern was not observed on the surface of microtubules, nor on what turned out to be intermediate filaments, as will be discussed below. Pure freeze-dried actin showed an identical "striped" pattern (J. E. Heuser and R. Cooke, manuscript in preparation). Thus this pattern may reflect the underlying 55-Å repeat of the monomers that compose the actin filaments.

As shown in Fig. 3, similar filaments could be seen running individually between adjacent stress fibers and helter-skelter in the coarse meshwork above the stress fibers. Many of these, having the same thickness as the ones in bundles, nevertheless looked whiter and did not display the striped granular pattern of platinum deposition as clearly. Presumably this was because, being unobstructed by other structures, they received a heavier platinum deposit.

Unfortunately, the double helical pattern of the actin filament has not so far been visible in our replicas of freeze-dried pure actin, nor in the 95-Å filaments we see in cytoskeletons. Nevertheless, this helix could be brought out dramatically by decorating these filaments with S1, the head fragment of the myosin molecule, which binds stereospecifically to actin. (This result was part of a collaborative effort, conducted with R. Cooke, that, will be reported in detail elsewhere, to visualize actin-myosin interaction.) Cytoskeletons soaked in S1 for 10 min after extraction with Triton no longer displayed any 95-Å, vaguely striped filaments. Instead, essentially all of the filaments in the stress-fiber bundles, and many of the filaments in other regions, were thickened to ~220 Å and looked clearly like double helices (Fig. 7). These helices were also vaguely striped, with foci of platinum grains spaced every 55 Å, which may have corresponded to the individual S1 molecules. An identical pattern was observed after purified skeletal muscle actin was decorated with S1 (J. E. Heuser and R. Cooke, manuscript in preparation).

Interestingly, not all the filaments in cytoskeletons such as that in Fig. 7 become decorated with S1. Some remained thin and uniform. These undecorated filaments typically occurred in between the bundles of filaments and often ran at right angles to the bundles, thus forming a "woof" in the skeletons' filamentous actin "warp". Subsequent observations described below confirmed that these were intermediate filaments, and not actin.

Further confirmation of the filament types could be obtained by selective extraction. As shown in Fig. 4, in the absence of glycerol, tubulin was extracted as judged by immunofluorescence and as shown in Fig. 8 by gel electrophoresis (cf. slots *2* and *3*). Microtubules were not found ultrastructurally in the glycerol-free cytoskeletons. Similarly, we could confirm that the bundles of filaments were composed primarily of actin, by extracting actin from cytoskeletons and observing the residue

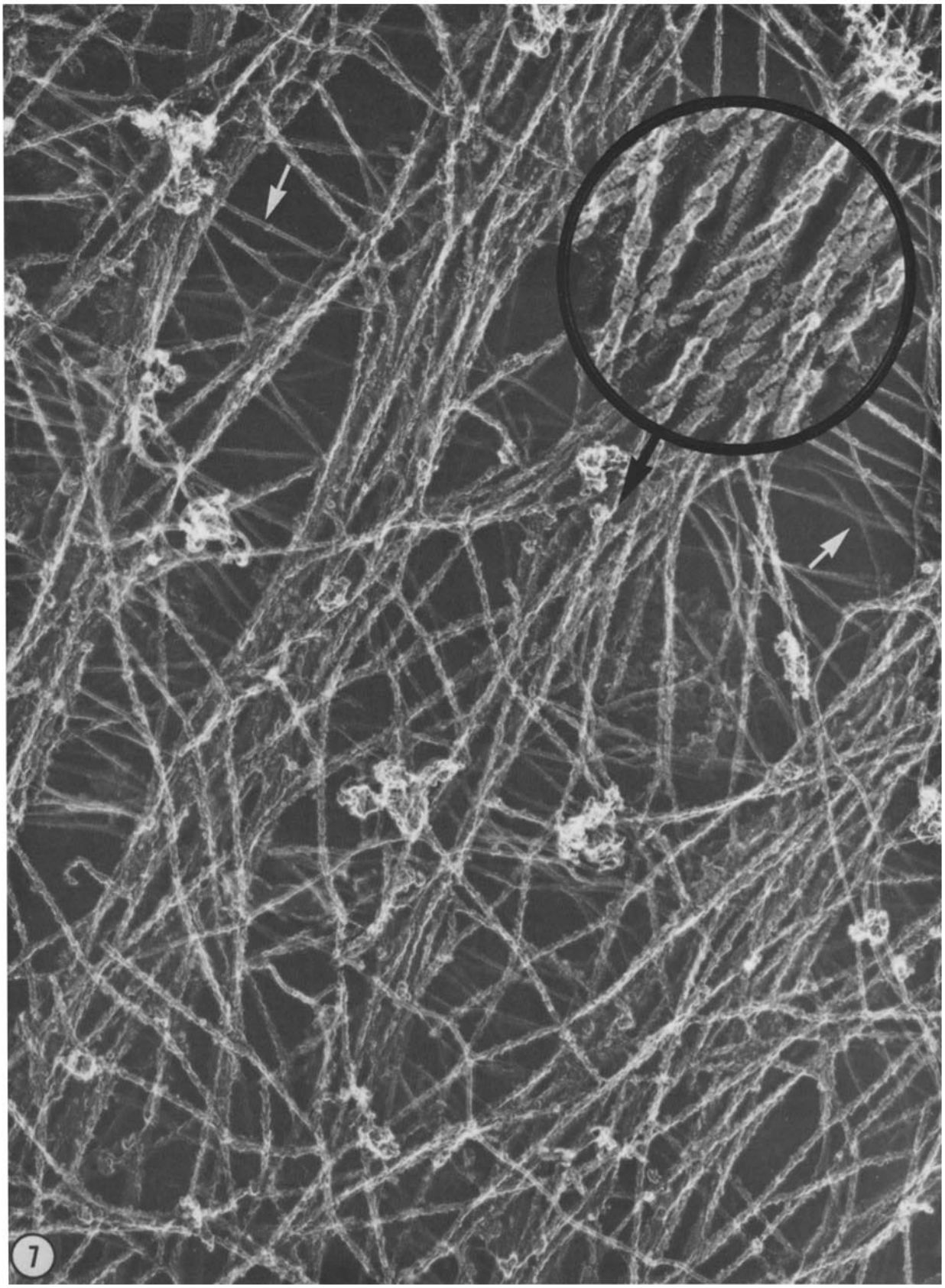

FIGURE 7 Replica of a freeze-dried cytoskeleton that was exposed to the myosin subfragment 1 (S1) before quick-freezing. Nearly all the filaments in the lengthwise bundles, and many of the intervening filaments, have been thickened and converted into ropelike double helices (see *inset*). However, some of the filaments that travel by themselves, in between the bundles, remain totally undecorated (arrows); these are presumably intermediate filaments. × 70,000; *inset*, × 200,000.

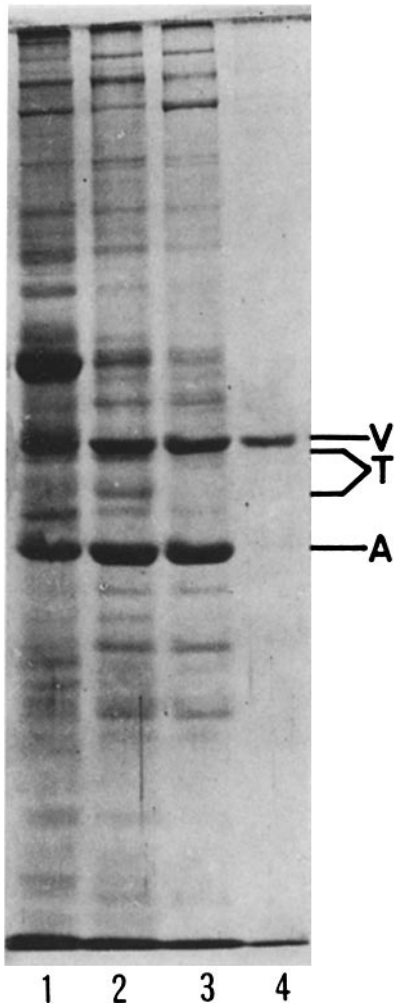

FIGURE 8 Gel electrophoresis of isolated cytoskeletons. The position of vimentin (58,000-dalton intermediate filament protein) is denoted by *V*, the tubulin dimer by *T*, and actin by *A*. Shown in slot *1* is the complete repertoire of proteins found in whole mouse embryo fibroblasts grown in tissue culture (including an intense band at 68,000, which is serum albumin from the culture medium). Shown in slot *2* are Triton cytoskeletons prepared in glycerol, which display a prominent tubulin band as well as actin and vimentin bands. Shown in slot *3* are Triton cytoskeletons prepared in the absence of glycerol, which results in loss of microtubules and leaves only actin and vimentin as the prominent bands. Shown in slot *4* is the residue that remains after 0.3 M KI extraction, which is composed almost exclusively of 58,000-dalton protein. The electrophoresis was done in an 8.5% acrylamide gel, using the procedure of Laemmli (17).

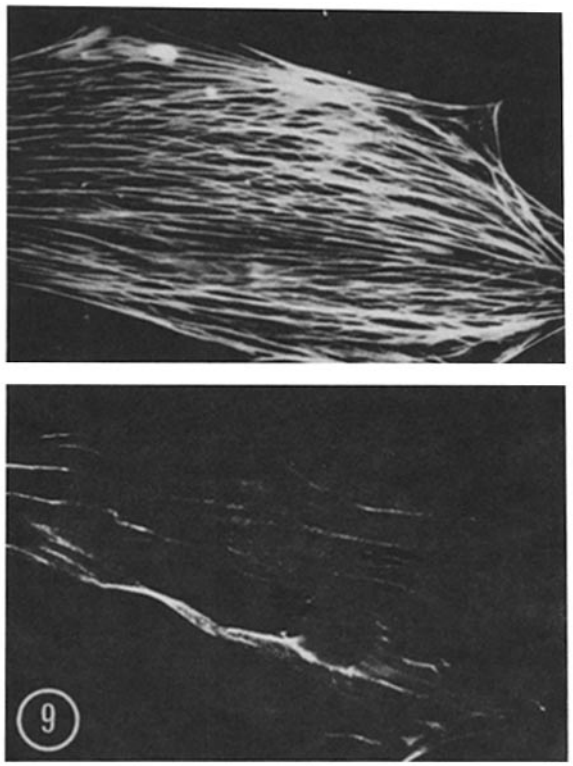

FIGURE 9 Anti-actin immunofluorescence of a mouse fibroblast cytoskeleton prepared by Triton extraction in glycerol-free stabilization medium (top) compared with the immunofluorescence of a fibroblast cytoskeleton treated with 0.3 M KI for 3 h to remove actin (bottom). × 1,250.

ultrastructurally. Actin extraction was accomplished by exposing cytoskeletons to 0.3 M KI for 3 h or exposure to pancreatic DNase I (14). This removed >80% of the actin, as determined by gel electrophoresis. For example, slots *3* and *4* on the gels displayed in Fig. 8 show the proportion of actin vs. vimentin (intermediate filament or 58,000-dalton protein; see for example reference 11), in skeletons before and after extraction with KI. Note that after extraction, the actin band largely disappeared, leaving the vimentin band as the principal component. This removal of actin was confirmed by staining the cells with antibody to actin using indirect immunofluorescence. Fig. 9 shows actin localization in an unextracted cytoskeleton. The actin showed its typical localization into bundles that course the length of the cell (19). After extraction with KI, only a faint, diffuse fluorescence remained, yet the cells retained their nuclei and general contour. Similarly, cytoskeletons freeze-dried and rotary replicated after KI extraction (Fig. 10) possessed only ragged remnants of their stress fibers, further confirming that actin was one of the major components of these structures. The remaining filaments were smooth surfaced and distinctly thicker (115 ± 10 Å) than were actin filaments after shadowing. Such 115-Å filaments could also be seen in the original untreated skeletons, whether aldehyde fixed or not. They could be distinguished from the 95-Å presumptive actin filaments not only by their thickness, but also by their smooth surface and by the general course they took through the cytoskeleton. They seemed to curve more gently, bend less often at points of intersection, and form bundles much less frequently than the actin filaments, all of which suggested that they were stiffer than actin.

To substantiate that the 115-Å filaments in these replicas represented intermediate filaments coated with a thin layer of platinum, cytoskeletons were next decorated with antibody to intermediate filament protein (kindly provided by Richard Hynes, who obtained it by immunizing rabbits with the 58,000-dalton protein from hamster cells [16]). By indirect immunocytochemistry (Fig. 11), it was clear that this antibody stained a filament network different from the stress fiber–actin system or the microtubule system (compare Fig. 11 [top] with Figs. 4 [top] and 9 [top]). Fig. 11 (bottom) illustrates that this antibody staining was not altered by extraction with 0.3 M KI, a treatment that substantially removed actin-containing structures.

Examination of cytoskeletons frozen and freeze-dried after decoration with the anti-58,000-dalton antibody (Fig. 12) con-

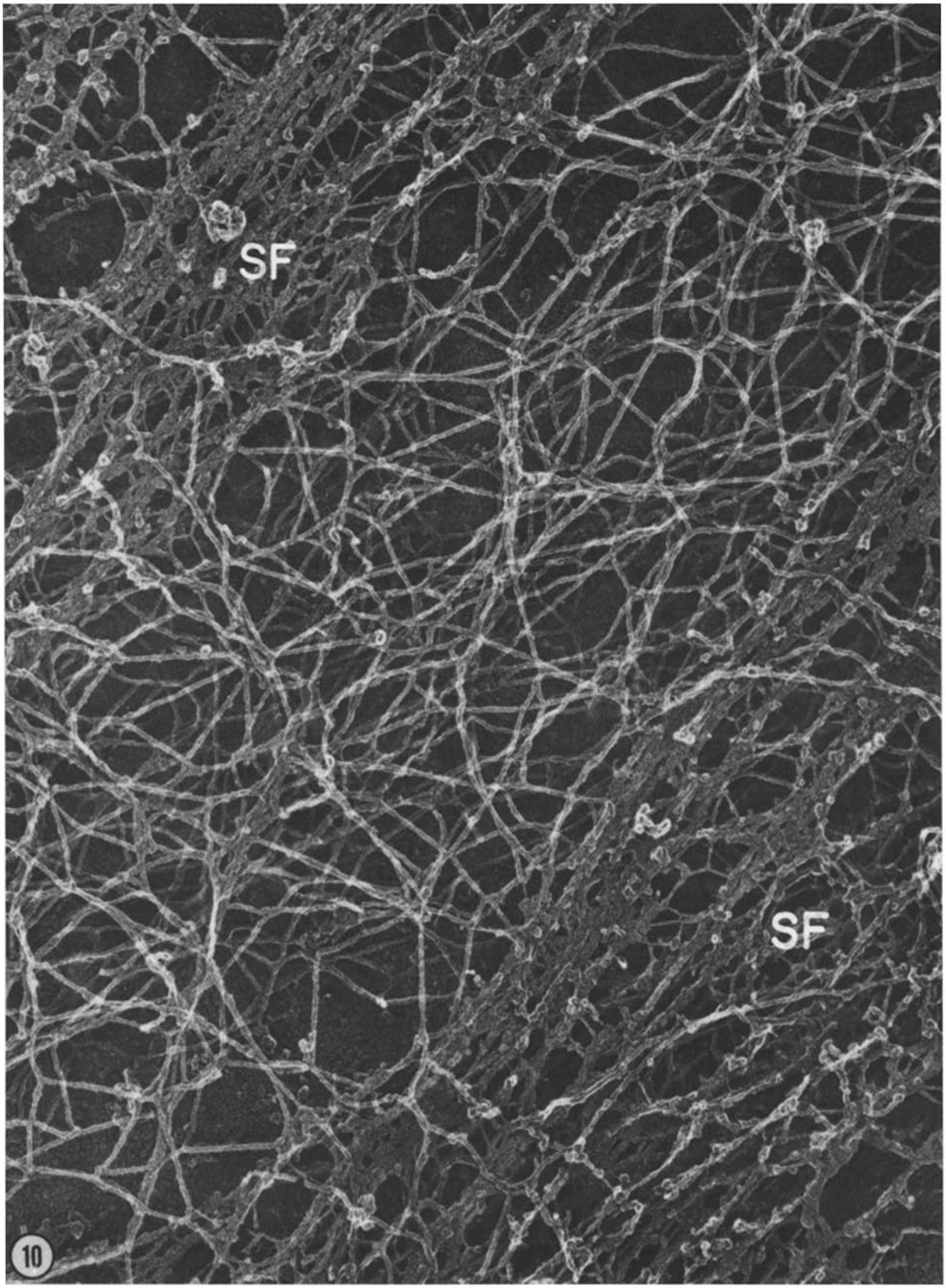

FIGURE 10 Replica of a freeze-dried cytoskeleton that was extracted with 0.3 M KI for 1 h before freezing. This removed ~80% of the actin, according to gel electrophoresis, and has severely disrupted the longitudinal bundles of filaments, which now resemble ragged coagulums (at *SF*). Left behind, however, is a rich network of filaments in between the damaged stress fibers, presumably equivalent to the 58,000-dalton intermediate filament protein left on gels. × 70,000.

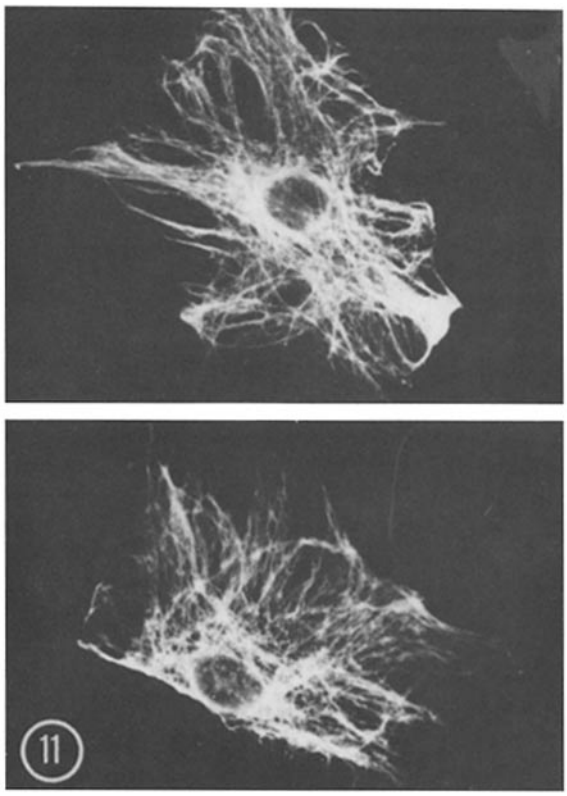

FIGURE 11 Anti-vimentin immunofluorescence of a mouse fibroblast cytoskeleton prepared by Triton extraction in glycerol-free stabilization medium (top) and a cytoskeleton extracted with 0.3 M KI (bottom), showing that KI does not remove the vimentin filaments when it removes the actin. × 1,000.

firmed that it was reacting with a type of filament different from actin. Gone were the smooth, individual filaments that were normally woven between the actin bundles; in their place were thick, coarsened strands measuring 285 Å on the average. These coarsened filaments were presumably intermediate filaments that had been coated with a knobbly layer of antibody molecules. Although antibody decoration of intermediate filaments did not look nearly as orderly as S1 decoration of actin filaments, it did unambiguously localize these filaments on the ultrastructural level. In addition, it showed that antibody-antigen association could be visualized directly by this technique of tissue preparation and replication.

In summary then, the freeze-dry rotary-replica technique appeared to be suitable for distinguishing—in addition to microtubules—the two types of filaments that remain in cytoskeletons of mouse fibroblasts after Triton extraction: actin and vimentin. Fig. 13 illustrates this distinction by displaying four fields of decorated and undecorated filaments at the same high magnification. Fig. 13 *a* and *b* are from freshly plated fibroblasts that did not have time to spread out or form stress fibers, and stained diffusely with anti-actin antibodies. They could be seen to contain an isotropic mesh of 95-Å filaments that intersected and overlapped, but did not branch or anastomose. These filaments looked coarsely granular and vaguely striped in platinum replicas and, when decorated with S1, formed distinct "ropes" (Fig. 13 *b*). They could therefore be identified as actin.

Fig. 13 *c* and *d*, on the other hand, were from old fibroblasts (plated at least 24 h before the experiment) whose actin was woven largely into stress fibers. In between these stress fibers was a meshwork of 115-Å filaments, shown in Fig. 13 *c*, that were distinctly thicker and less coarsely granular than the actin shown in Fig. 13 *a*. These intervening filaments became considerably thickened and knobbly when exposed to antivimentin antibody (Fig. 13 *d*). These, presumably, were intermediate filaments.

Patterns of Filament Organization

With the three major filament types found in cytoskeletons thus defined by chemical extraction, specific decoration, and morphology, it became possible to recognize the overall patterns in which these fibrous components of the protoplasm were woven together, and to recognize how these patterns changed when the cells changed shape. This analysis was aided by examining the cytoskeletons in stereo. The patterns shown so far in Figs. 3, 7, 10, and 12, in which distinct actin bundles were woven together by individual actin and vimentin filaments, was typical only of the thinner regions of older cells. Occasionally, in the thicker regions of older cells, these bundles of filaments appeared to radiate out from starlike foci (Fig. 14). These were presumably the vertices of the "geodesic domes" of actin (18) discovered in such cells by immunofluorescent staining. Less focused arrays were usually found in the thicker regions of these cells, and in younger cells that had not been allowed to spread so thin. Indeed, in round cells, which stained diffusely with anti-actin antibodies, actin filaments appeared to be distributed randomly and isotropically, as shown in Fig. 13, just as they were in pure actin gels.

The concentration of the actin filaments also appeared to vary in different parts of the cell. Around the nucleus, they were relatively sparse, and formed large interstices that may have accommodated relatively large membranous organelles. In thinner regions of the cell, they were often primarily bundled, as shown in Figs. 3, 7, 10, and 12. In the periphery, especially in the lamellopodia, the actin filaments were extremely concentrated. Fig. 15 illustrates this point. The top figure shows the outer surface of the cell membrane over an intact lamellopodium from a cell that was not extracted before freezing and drying. In the center is a lamellopodium with its membrane removed by treatment with Triton for 3 min before freezing. The extraction of the membrane by Triton exposed a dense network of filamentous strands that were characteristically striped, generally 95 Å in diameter, and capable of decoration with S1 (data not shown). It is well known from the work of Lazarides and Weber (19) that "ruffles" react strongly with anti-actin antibody. However, unlike actin filaments elsewhere, these filaments did not appear to extend continuously past points of intersection. Either they were very short or else they must have bent acutely at each junction. Thus, the lamellopodia appeared to contain actin in its most concentrated and most cross-linked state.

Comparison of Cytoskeletons with Intact Cells

Fig. 15 *c* also shows an image of a ruffle from a cell that was fixed, while intact, with glutaraldehyde and subsequently extracted with Triton. After this sort of preparation, the cytoplasmic matrix of cultured fibroblasts showed subtle but distinct differences from that seen in cytoskeletons that were extracted first and fixed later. In thin ruffles, for example, the delicate web of actin that was retained in the cytoskeleton (Fig. 15 *b*) was coarsened and partly obscured by aldehyde fixation (Fig. 15 *c*). This appeared to be the result of lateral aggregation

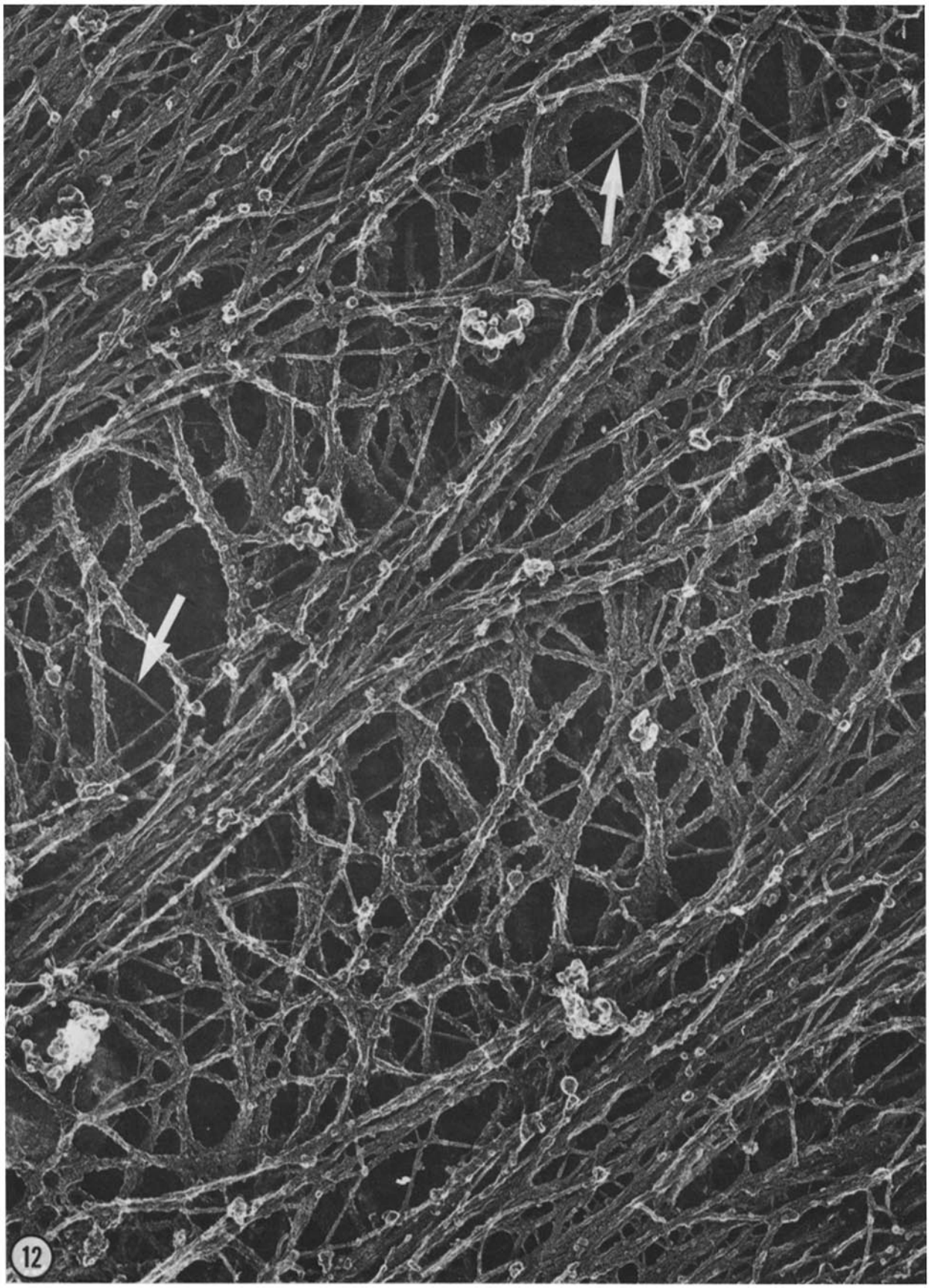

FIGURE 12 Replica of a freeze-dried cytoskeleton exposed to antibodies against intermediate filaments before quick-freezing. The filaments that form the longitudinal bundles do not appear to be altered, but the filaments that compose the intervening loose networks appear, for the most part, to be grossly thickened. A few thin, undecorated filaments persist in these areas (arrows); presumably, they were individual actin filaments. × 70,000.

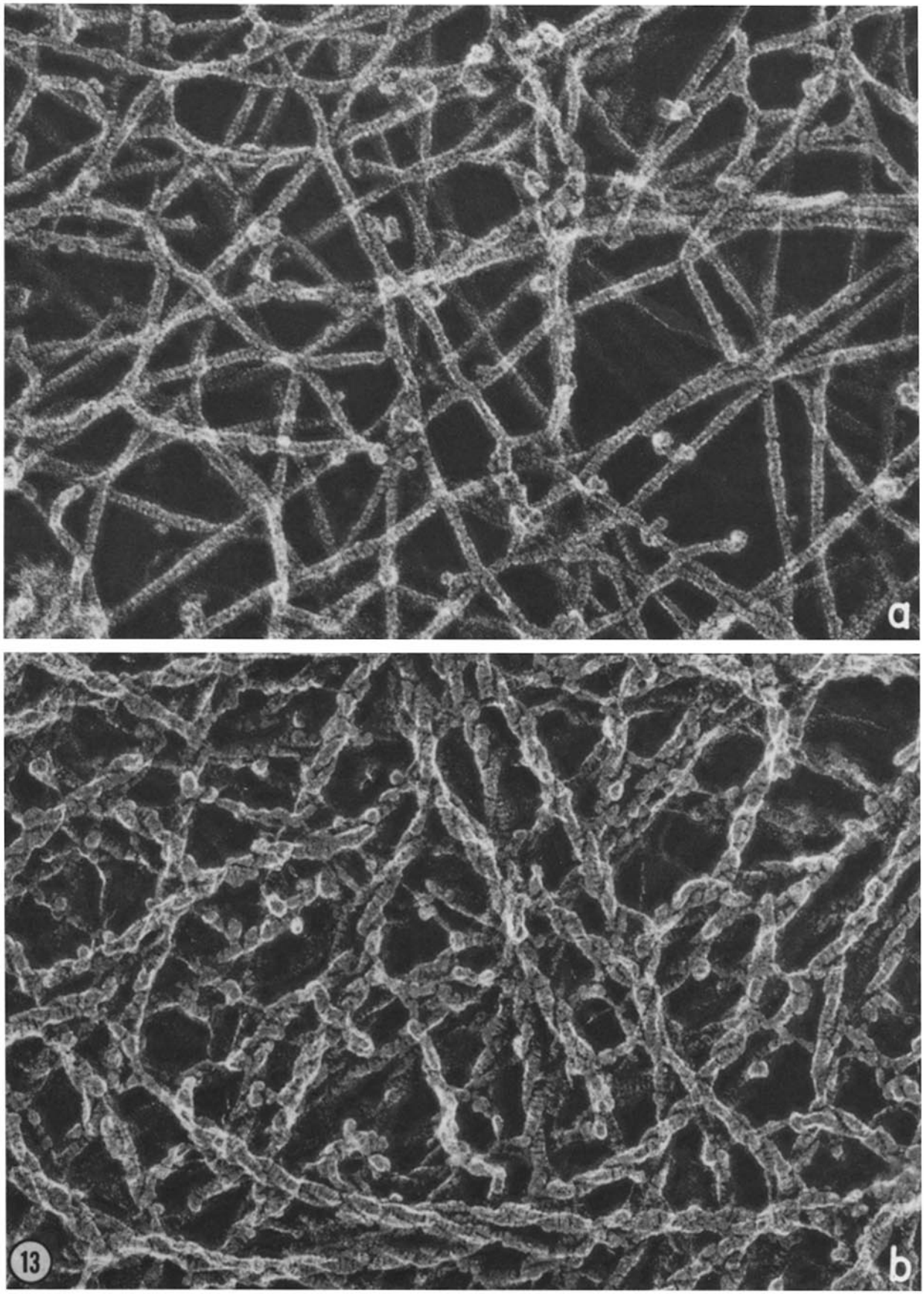

FIGURE 13 Four higher-magnification views of cytoskeletal filaments under different conditions, all printed at comparable magnification to facilitate direct comparison. *a* is a tangle of filaments from the perikaryal region of a freshly plated, somewhat round cell, which would stain diffusely for actin by light-microscope immunocytochemistry. The filaments are 95 Å in diameter and display a characteristic 55-Å surface roughness or graininess that appears to be pathognomic of actin filaments. *b* is a tangle of filaments from a region like *a*, after exposure to S1. As a result of this decoration, each individual filament appears to have

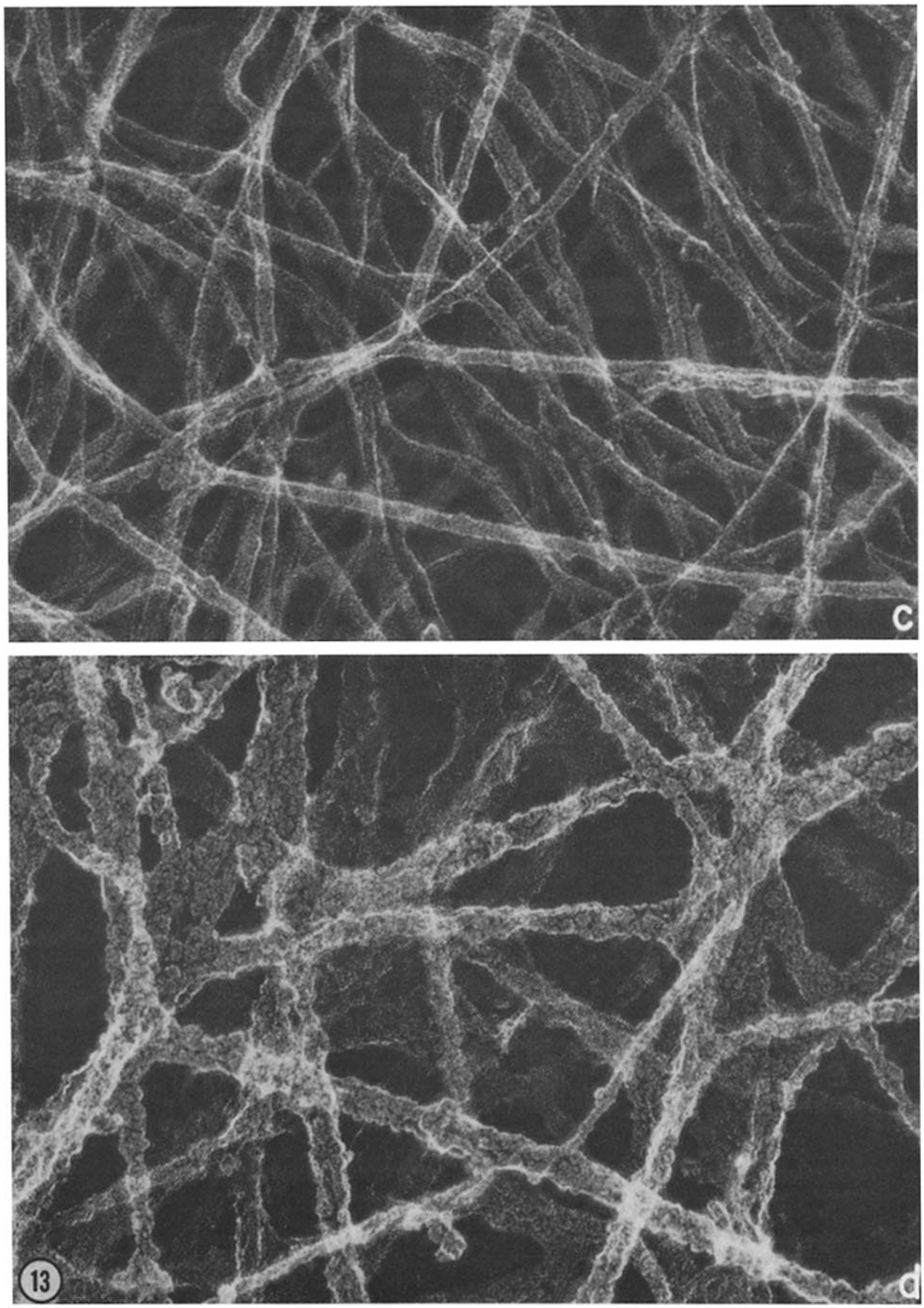

become a double-stranded "rope," in which each strand displays the 55-Å axial periodicity even more clearly than the underlying actin filament. *c* is a typical tangle of the filaments found in the regions in between stress fibers, where filaments are distinctly thicker than actin (115–120 Å vs. 95 Å for actin) and appear to be coated by a more uniform, less granular layer of platinum. *d* is an image of such "intermediate" filaments after exposure to antivimentin antibody. They become considerably thickened and knobbly, as a result of what must be an adhering layer of antibody molecules.

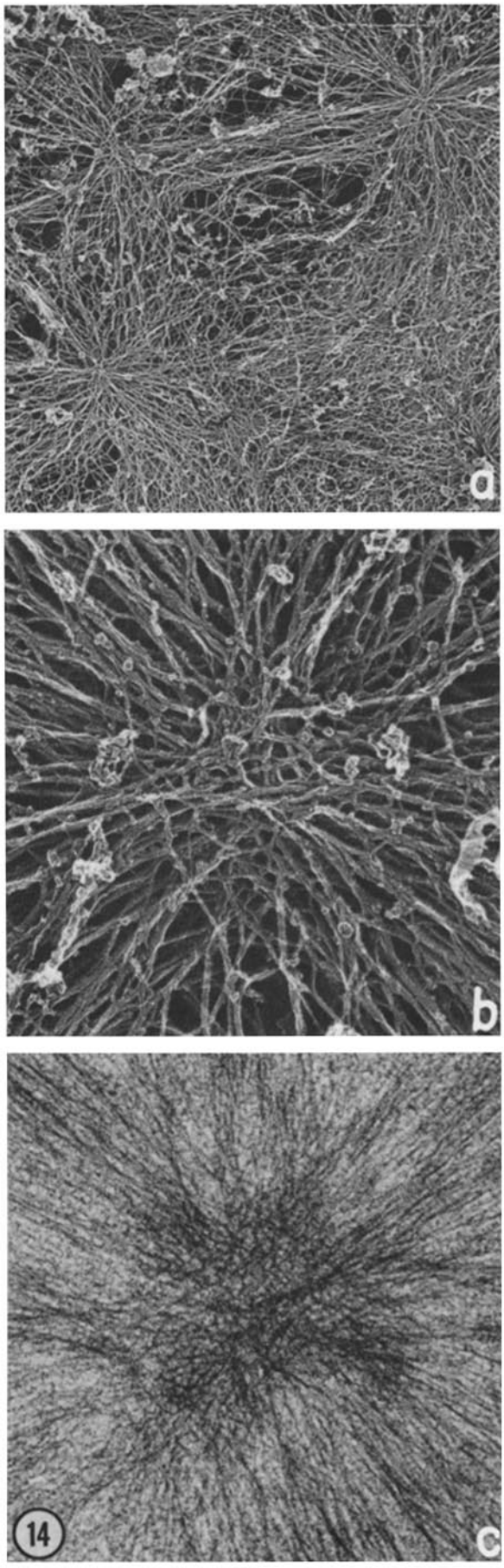

of the individual filaments and of adherence of lumpy material to the aggregated filaments.

Lower magnification survey views of the thinner parts of these fixed and subsequently extracted cells, such as that in Fig. 16 (which is displayed at the same magnification as the previous Figs. 3, 7, 10, and 12, for ready comparison), confirmed the impression that the same filamentous components were present in fixed whole cells as in the cytoskeletons; but after fixation, the various filaments were partly agglutinated and partly obscured by adhering material. This made them look more branched, more anastomotic, more variable in thickness and, in short, more like a "trabecular meshwork" than they looked in the isolated cytoskeleton.

Which image was more real, i.e., more true to nature, was not easy to decide. One might have hoped that simply fracturing whole cells open and deep-etching them, without ever fixing them, would reveal the true nature of the organization of their cytoplasm. Unfortunately, the whole cell turned out to be so loaded with nonvolatile material that it was almost like looking at a thin section, and very little depth could be seen. Unidentified granular material filled in everywhere and largely obscured the view, and little could be learned about the pattern of filament organization.

The only way we could expose a reasonable number of the filaments inside the intact cell was to swell the cell by placing it briefly in distilled water, and thus partially diluting its contents before freezing. Fig. 17 illustrates a representative region from such a swollen cell. The fracture broke partly through a filament bundle in the center of the field and, in addition, exposed a number of individual filaments on either side of the bundle. But in spite of the swelling, a large amount of granular material still obscured the filaments and prevented us from determining much about their overall organization.

DISCUSSION

The method introduced here for preparing cytoskeletons for electron microscopy achieves two major requirements for visualizing the filamentous systems in cells. First, it combines sufficient resolution to identify the filament types by their morphology alone. Second, it can be used with whole mounts of cells to give the realism and perspective of three-dimensional visualization. Using this method we have illustrated that the cytoskeleton of primary mouse embryo fibroblast cells is composed of discrete actin filaments, intermediate filaments, and microtubules woven into characteristic bundles and networks.

Identifying the Filaments

In general, filaments were identified by their specific morphology. For example, microtubules not only displayed their characteristic surface protofilament structure, but also revealed for the first time in fractured samples the structure of their interior. Their luminal wall was seen to have a prominent 3-start helical arrangement of subunits, quite distinct from the

FIGURE 14 Three views of the foci of filament convergence that may represent the vertices of the actin "geodomes" seen in fibroblasts by light-microscope immunocytochemistry (18). Superficially, the centers of these foci have filaments running into them like the Z-bands of muscles, both when viewed in freeze-dried replicas (*b*) and when viewed in freeze-substituted whole cells (*c*). (*a*, × 10,000; *b* and *c*, × 65,000).

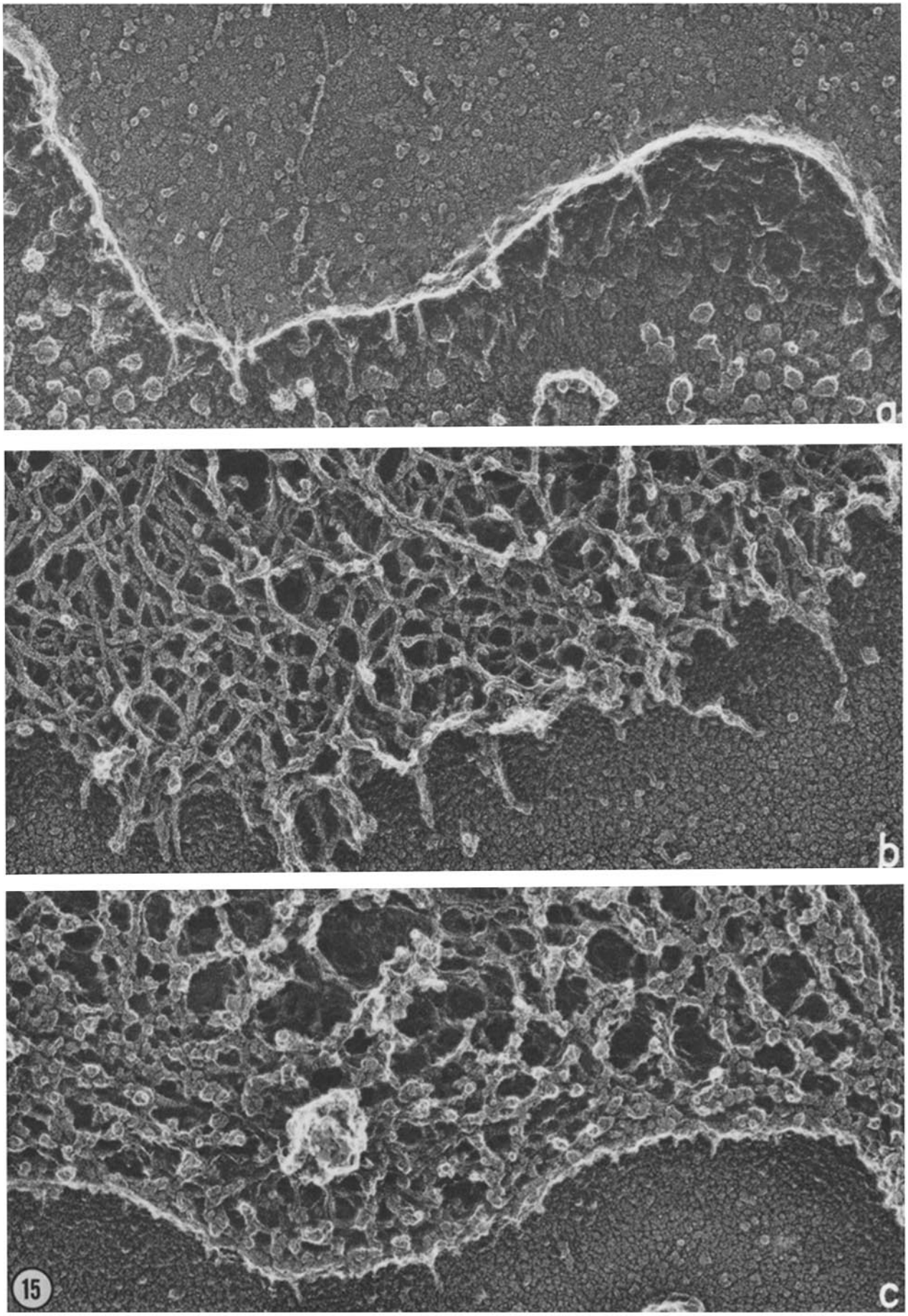
a
b
15
c

prominent 13-stranded protofilament structure of their outer surface. Similarly, actin filaments displayed a characteristic surface granularity with a repeat at approximately every 55 Å, which hinted at their basic construction from 55-Å G-actin monomers. Of course, there was no way to know whether the details visible in such platinum replicas were an accurate reflection of the real surface contours of these macromolecules or whether they were actually some sort of "decoration" phenomenon resulting from an irregular disposition of platinum on the underlying structures. In any case, these substructural details were visible on all the replicas and allowed us to distinguish one filament type from another. For example, the 55 Å granularity seen in actin filaments was quite unlike the smooth deposit of platinum that formed on the slightly thicker filaments later identified as intermediate filaments.

Secondly, the filaments were identified by selective extraction. Conditions of extraction could be altered in such a way that the cytoskeletons no longer reacted with antibodies to a particular filament as viewed in the fluorescence microscope and no longer displayed that protein by gel electrophoresis. These samples were also freeze-dried and examined in the electron microscope to see which filament type was missing. With microtubules, this was particularly easy. Simply omitting glycerol from the original Triton extraction medium caused them to disappear completely. They were only stable in the absence of glycerol when 10^{-6} M Taxol was present. Actin was a little harder to extract, but could be substantially removed, as determined by gel electrophoresis and immunocytochemistry, by exposing the cytoskeletons to 0.3 M KI for 3 h. This treatment removed the stress-fiber bundles and the ruffles from the freeze-dried cytoskeletons, but left a remarkably dense residuum of filaments. These were the filaments that looked slightly thicker and smoother than actin filaments. Gel electrophoresis illustrated that the only major cytoplasmic protein left after these treatments was the 58,000-dalton subunit of intermediate filaments recently named vimentin (11).

A third way of identifying the filaments in cytoskeletons was by specific decoration. Actin filaments were identified by exposing cytoskeletons to the myosin subfragment S1, which on binding drastically changed the appearance of the actin filaments. A characteristic "ropelike" double-stranded helix was produced that is apparently equivalent to the familiar "arrowhead" image of decorated actin seen by Huxley (15) after negative staining. (Elsewhere, we will evaluate the differences between these two images; J. E. Heuser and R. Cooke, manuscript in preparation.) Intermediate filaments were identified by exposing cytoskeletons to specific antibodies against the 58,000-dalton intermediate filament protein. These antibodies decorated a significant proportion of the filaments in the cell and specifically those that did not react with S1. Unlike the results of S1 binding to actin, the coat of antibodies was too thick and irregular to reveal any underlying order that might have existed in the intermediate filament surface lattice. Nevertheless, it was apparent that the freeze-dry replica method had sufficient resolution to visualize antigen-antibody complexes directly, without the need for additional electron-dense tags that are usually used in electron microscope immunocytochemistry.

The Organization of Cytoskeletons

The most important conclusion that has emerged from this new preparative technique so far has been a simple one; namely, that cytoskeletons are composed almost entirely of discrete filaments. This is not a novel observation; it only confirms what has been said before on the basis of negative-stain images (4, 26). However, it does not coincide exactly with the transmission electron microscope views of cytoskeletons obtained by positive staining and critical-point drying (28). Cytoskeletal components are translucent after such preparation. When they overlap each other, their images become more difficult to interpret than images of filaments in opaque replicas or in negative stain. With the help of stereomicroscopy to sort out overlapping structures, it has become clear that individual components in critical-point-dried skeletons look both "trabecular" and filamentous. Parts of the images show structures of variable thickness, which merge at truncated intersections and look a bit more like the walls of a sponge than the strands of a web (28). Indeed, the critical-point-dried skeletons look in some respects similar to the images of critical-point-dried protoplasm seen inside whole cells viewed by stereo high-voltage electron microscopy, which Wolosewick and Porter (32) have described as a "microtrabecular meshwork."

Comparison of Cytoskeletons and "Microtrabeculae"

The appearance of the platinum replicas of freeze-dried cytoskeletons is different in important ways from the views of conventionally fixed and stained cytoskeletons and the views of unextracted cells seen by high-voltage electron microscopy. The latter two techniques and particularly high-voltage electron microscopy suggest that the cytoplasm is composed of a three-dimensional lattice of formed elements, the microtrabeculae, which support filaments and organelles and pervade every nook and cranny of the cytoplasmic space. (31, 32). These microtrabeculae appear to vary in thickness and to fuse with each other at points of intersection. They appear also to merge imperceptibly with a thin cytoplasmic "matrix" that coats microtubules and all membranes after aldehyde fixation. In contrast, the cytoskeleton seen after freeze-drying appears to be composed of nothing but discrete filaments of uniform caliber, which crisscross each other in complex patterns but do not appear to fuse. In whole freeze-fractured cells, these filaments appear to lie embedded in a granular cytoplasmic matrix but do not appear to fuse with microtubules or with the membranes of cell organelles.

These fundamental differences in appearance raise the question: Are microtrabeculae additional components superim-

FIGURE 15 Three moderately high powered views of ruffles or lamellopodia from fibroblasts that were fixed while whole (in *a*), were extracted with Triton before fixation (in *b*), or extracted with Triton after fixation (in *c*). In *a*, plasma membrane is intact and no internal structure can be seen. In *b*, the plasma membrane has been removed and an underlying web of "kinky" filaments revealed. In other experiments, these filaments decorate with S1, but they are much more concentrated and much more extensively interdigitated than actin in other regions of the cell. In *c*, the plasma membrane has again been removed, but only after the cell was fixed with aldehyde. The delicate meshwork of underlying filaments appears coarser after the chemical fixation. (*a*, × 140,000; *b* and *c*, × 115,000).

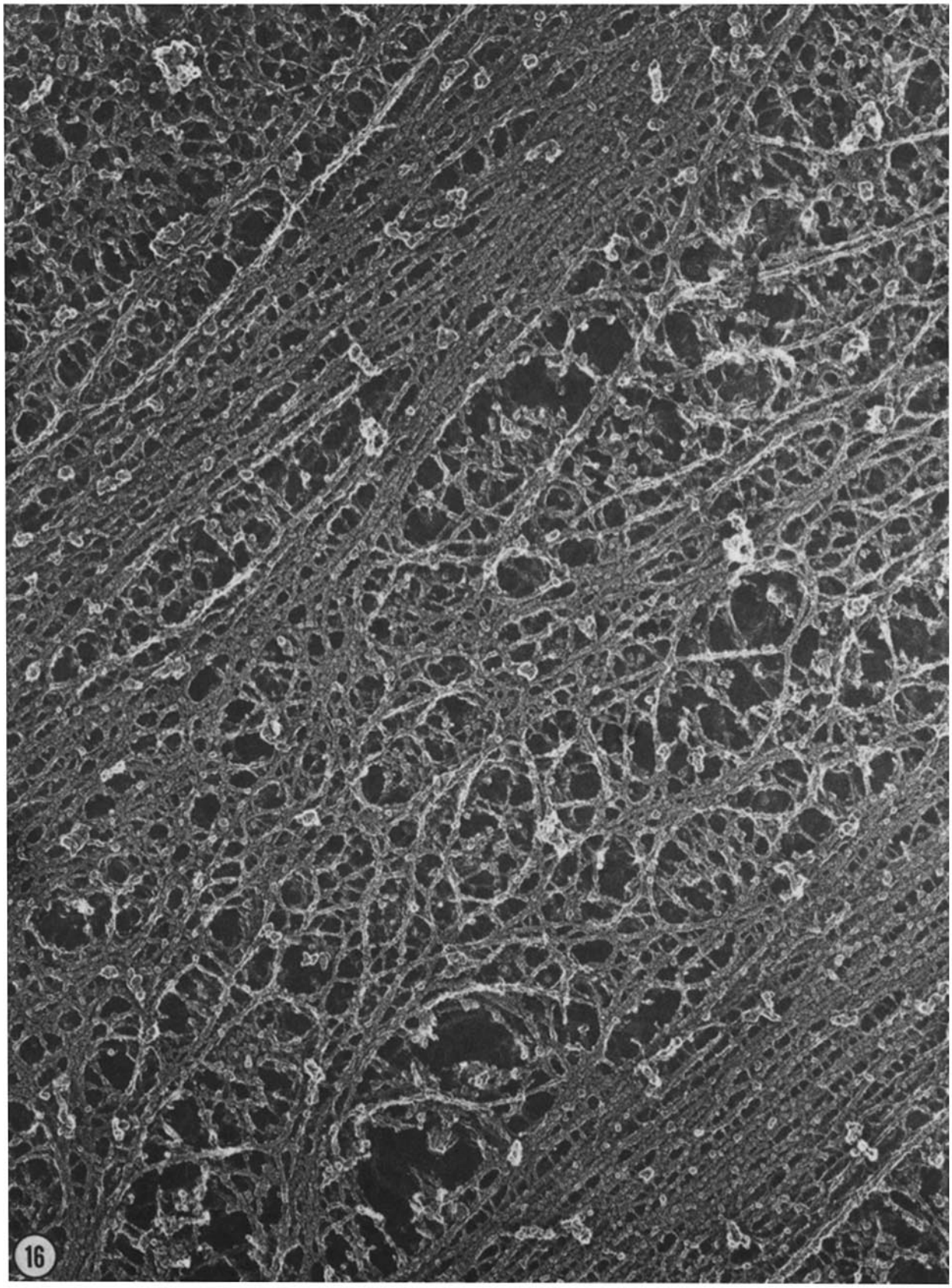

FIGURE 16 Replica of freeze-dried fibroblast that was fixed with aldehyde before extraction with Triton. Triton was still able to remove the membrane and expose the cytoplasmic matrix. It is no longer easy, however, to discern individual filaments therein, except in the obvious stress fibers (*SF*). Instead, the whole matrix looks more like a continuous spongework of curvilinear elements with smoothly varying diameters, not unlike the "microtrabecular meshwork" seen in whole cells by high-voltage electron microscopy. × 70,000.

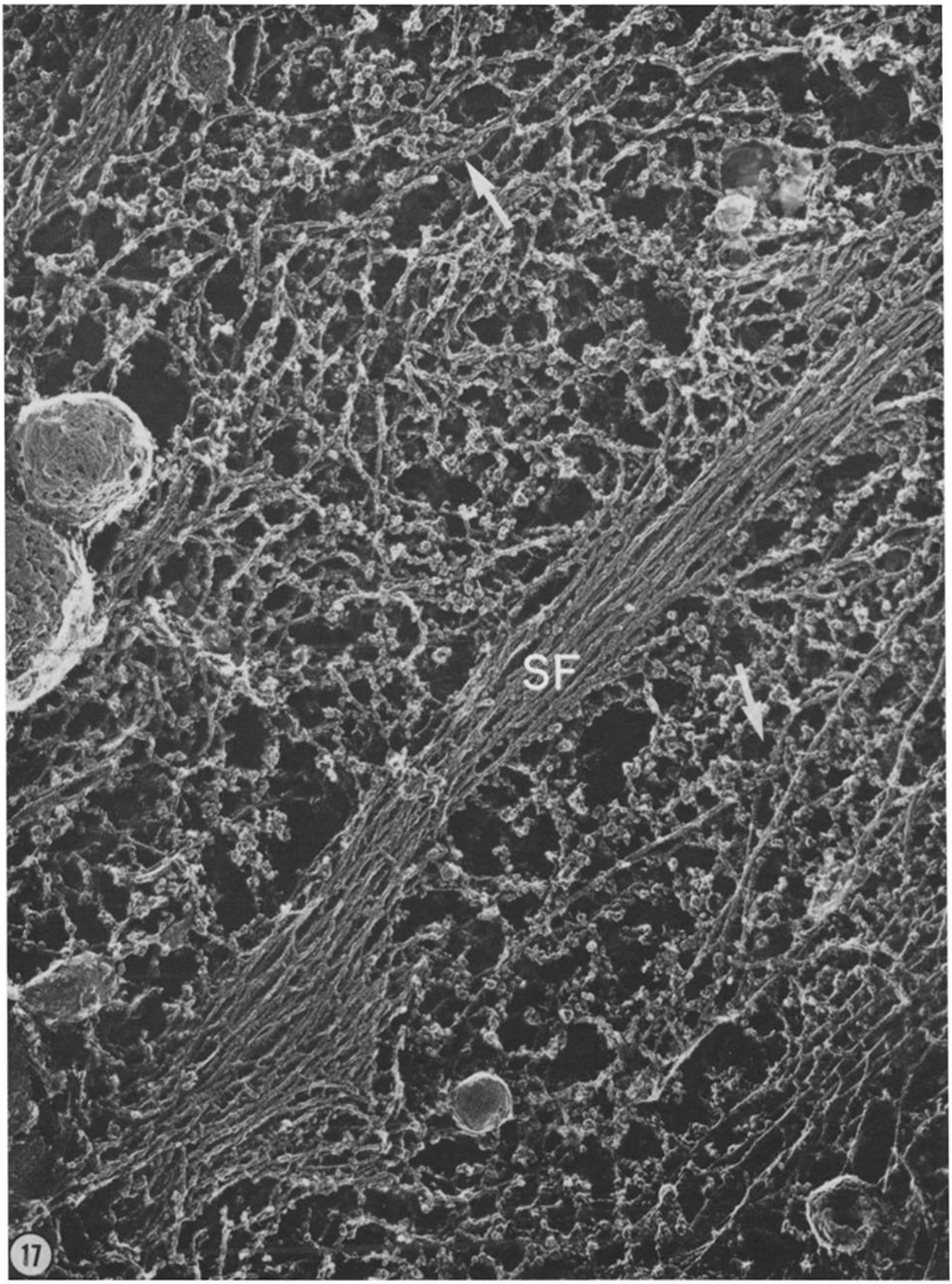

FIGURE 17 Replica of an intact fibroblast that was swollen in distilled water for 1 min before freezing. It was then freeze-fractured and deep-etched for 3 min at −100°C, rather than Triton extracted and freeze-dried. Though cytoplasmic filaments are less readily discernable in whole cells, as a result of the granular material that fills all areas, at least one stress fiber bundle (*SF*) and a number of individual filaments (arrows) can be seen. A disappointing aspect of these views was that the granular material (presumably soluble cytoplasmic protein) obscured so much that it was impossible to tell whether the whole cell might possess microtrabeculae that were not seen in the cytoskeletons. × 70,000.

posed on the cytoskeleton of actin, intermediate filaments, and microtubules, components that are extracted and therefore not visualized in cytoskeletal preparations; or is the microtrabecular lattice a different sort of image of the same cytoskeletal filaments we see in freeze-dried cells?

We favor the latter explanation. For example, in the lamellopodia where high-voltage electron microscope images reveal nothing but microtrabeculae (31), the current method resolves a dense tangle of individual actin filaments that are no less concentrated than the microtrabeculae (maximum separation, 500 Å). Nor is there any indication, at any other locus in the cell, that microtrabeculae form a finer mesh than the components of the cytoskeleton.

However, before we could conclude that the microtrabeculae are essentially cytoskeletal filaments, we would have to show how the filaments could end up looking like trabeculae after fixation, staining, and critical-point drying. To do this, we quick-froze and deep-etched whole cells after each step in such a preparative procedure. This illustrated that discrete filaments abound in the cytoplasm of unfixed cells, but that after aldehyde fixation, these filaments appear to be, by comparison with unfixed cells, partially agglutinated and decorated with irregular condensations of what may have been soluble cytoplasmic proteins. This was illustrated above by comparing Fig. 15 *c* with *b*, or Fig. 16 with Fig. 3. After fixation, organized structures such as actin bundles could still be distinguished, but individual actin fibers became impossible to recognize.

Subsequent alcohol dehydration caused further collapse and coarsening of these cross-linked cytoplasmic components. The final image looked very much like the microtrabeculae seen in high-voltage electron microscopy. Thus, from these studies, we believe that microtrabeculae are actually a different image of the individual actin and intermediate filaments that normally weave among the other formed components of the cytoplasm. It seems that after these filaments become agglutinated and decorated with other cytoplasmic proteins during aldehyde fixation, they appear as curvilinear struts in a confluent trabeculum, rather than discrete filaments woven into a complex fabric.

Future Applications

The high-resolution surface views provided by these platinum replicas have permitted us to sort out the overlapping filaments and identify them individually by their characteristic diameters and surface features. Thus, this method of viewing bridges the gap between the scanning electron microscope view of cellular shape and the negative stain view of molecular shape. It reveals detail at the macromolecular level, with a minimum of distortion, and is directly applicable to whole mounts of cells or cell organelles. We hope that in the future, with improvement of the vacuum evaporation of thin films, the technique can reach beyond the present level of resolution, and thus provide a three-dimensional surface view of molecules that would overcome some of the limitations of negative staining, such as opacity of large structures, collapse upon drying, and superimposition of the opposite sides of structures.

Nevertheless, at the present level of resolution, the surface-replica technique has already proved useful for visualizing changes in cytoskeletal organization that relate to changes in cell function. We have already learned, for example, that the loss of stress fibers and a rounding up that occurs during cell transformation is accompanied by a shift of a large proportion of the actin filaments in the cytoskeleton from a bundled state to a randomly interwoven state. Even though the perinuclear cytoplasm of transformed cells appears, by light microscope immunocytochemistry, to stain diffusely for actin, this new technique has the resolution to show that actin is still filamentous in these areas and has only become rewoven into a diffuse, isotropic three-dimensional mesh.

This technique has not yet revealed any indication of where or how the tangled filaments are cross-linked. No specializations or discontinuities can be seen at the points of intersection, so it is impossible to know which are mere contact and which are real bonds. Thus, it remains to be seen whether the filaments that make up cytoskeletons are extensively cross-linked to each other. Because this technique can visualize antibody molecules directly without secondary labels, its use with specific antibodies to structural proteins, such as α-actinin, desmin, tropomyosin, myosin, tau, and HMW, should allow a reconstruction, at the ultrastructural level, of the organization of the fibrous systems of the cell.

We thank Louise Evans and Margaret Lopata for excellent technical help during the course of these experiments. Further, we wish to thank Roger Cooke for the gift of the S1, Robert Pollack and Keith Burridge for the gift of the anti-actin antiserum, and Richard Hynes for the gift of the antivimentin antiserum. We thank Susan Horowitz (Albert Einstein College of Medicine, Bronx, N. Y.) for the kind gift of Taxol.

Received for publication 29 January 1980, and in revised form 18 March 1980.

REFERENCES

1. Amos, L. A., and A. Klug. 1974. Arrangement of subunits in flagellar microtubules. *J. Cell Sci.* 14:533–549.
2. Bell, P. B., M. M. Miller, K. L. Carraway, and J. P. Revel. 1978. SEM-revealed changes in the distribution of the Triton-insoluble cytoskeleton on Chinese hamster ovary cells induced by dibutyryl cyclic AMP. *Scanning Electron Microsc.* II:899–906.
3. Bershadsky, A. D., V. I. Gelfand, J. M. Svitkina, and I. S. Tint. 1978. Microtubules in mouse embryo fibroblasts extracted with Triton X-100. *Cell Biol. Int. Rep.* 2:425–432.
4. Brown, S., W. Levinson, and J. A. Spudich. 1976. Cytoskeletal elements of duck embryo fibroblasts revealed by detergent extraction. *J. Supramol. Struct.* 5:119–130.
5. Buckley, I. K. 1975. Three-dimensional fine structure of cultured cells. Possible implications for subcellular motility. *Tissue & Cell.* 1:51–72.
6. Burridge, K. 1976. Changes in cellular glycoproteins after transformation: Identification of specific glycoproteins and antigens in sodium dodecyl sulfate gels. *Proc. Natl. Acad. Sci. U. S. A.* 73:4457–4461.
7. Cande, W. Z., J. Snyder, D. Smith, K. Summers, and J. R. McIntosh. 1974. A functional mitotic spindle prepared from mammalian cells in culture. *Proc. Natl. Acad. Sci. U. S. A.* 71:1559–1563.
8. Connolly, J. A., V. I. Kalnins, D. W. Cleveland, and M. W. Kirschner. 1978. Intracellular localization of the high molecular weight microtubule accessory protein by indirect immunofluorescence. *J. Cell Biol.* 76:781–786.
9. Cooke, R. 1972. A new method for producing myosin subfragment-1. *Biochem. Biophys. Res. Commun.* 49:1021–1028.
10. Erickson, H. 1974. Microtubule surface lattice and subunit structure and observations on reassembly. *J. Cell Biol.* 60:153–167.
11. Franke, W. W., E. Schmid, M. Osborn, and K. Weber. 1978. Different intermediate-sized filaments distinguished by immunofluorescence microscopy. *Proc. Natl. Acad. Sci. U. S. A.* 75:5034–5038.
12. Grimstone, A. V., and A. Klug. 1966. Observations on the substructure of flagellar fibres. *J. Cell Sci.* 1:351–362.
13. Heuser, J. E., T. S. Reese, M. J. Dennis, Y. Jan, L. Jan, and L. Evans. 1979. Synaptic vesicle exocytosis captured by quick freezing and correlated with quantal transmitter release. *J. Cell Biol.* 81:275–300.
14. Hitchock, S. E., L. Carlsson, and U. Lindberg. 1976. Depolymerization of F-actin by deoxyribonuclease I. *Cell.* 7:531–542.
15. Huxley, H. E. 1963. Electron microscope studies on the structure of natural and synthetic protein filaments from striated muscle. *J. Mol. Biol.* 7:281–308.
16. Hynes, R. O., and A. T. Destree. 1978. 10 nm filaments in normal and transformed cells. *Cell.* 13:151–163.
17. Laemmli, V. K. 1970. Cleavage of structural proteins during the assembly of the head of bacteriophage T4. *Nature (Lond.).* 227:680–685.
18. Lazarides, E. 1975. Immunofluorescence studies on the structure of actin filaments in tissue culture cells. *J. Histochem. Cytochem.* 23:507–528.
19. Lazarides, E., and K. Weber. 1974. Actin antibody: The specific visualization of actin filaments in nonmuscle cells. *Proc. Natl. Acad. Sci. U. S. A.* 71:2268–2272.
20. Lenk, R., L. Ransom, Y. Kaufmann, and S. Penman. 1977. A cytoskeletal structure with associated polyribosomes obtained from HeLa cells. *Cell.* 10:67–78.
21. Osborn, M., and K. Weber. 1977. The detergent resistant cytoskeleton of tissue culture cells includes the nucleus and the microfilament bundles. *Exp. Cell Res.* 106:339–349.
22. Osborn, M., and K. Weber. 1977. The display of microtubules in transformed cells. *Cell.* 12:561–571.

23. Raju, T. R., M. Stewart, and I. K. Buckley. 1978. Selective extraction of cytoplasmic actin-containing filaments with DNAse I. *Cytobiologie.* 17:307–311.
24. Schiff, P. B., J. Fant, and S. B. Horowitz. 1979. Promotion of microtubule assembly in vitro by Taxol. *Nature (Lond.).* 277:665–667.
25. Shelanski, M. L., F. Gaskin, and C. R. Cantor. 1973. Microtubule assembly in the absence of added nucleotides. *Proc. Natl. Acad. Sci. U. S. A.* 70:765–768.
26. Small, J. V., and J. E. Celis. 1978. Filament arrangements in negatively stained cultured cells: The organization of actin. *Cytobiologie.* 16:308–325.
27. Spiegelman, B., M. Lopata, and M. W. Kirschner. 1979. Multiple sites for the initiation of microtubule assembly in mammalian cells. *Cell.* 16:239–252.
28. Webster, R. E., D. Henderson, M. Osborn, and K. Weber. 1978. Three-dimensional electron microscopical visualization of the cytoskeleton of animal cells: Immunoferritin identification of actin and tubulin containing structures. *Proc. Natl. Acad. Sci. U. S. A.* 75: 5511–5515.
29. Webster, R. E., M. Osborn, and K. Weber. 1978. Visualization of the same PtK2 cytoskeletons by both immunofluorescence and low power electron microscopy. *Exp. Cell Res.* 117:47–78.
30. Weingarten, M. D., M. M. Suter, D. R. Littman, and M. W. Kirschner. 1974. Properties of the depolymerization products of microtubules from mammalian brain. *Biochemistry.* 13:5529–5537.
31. Wolosewick, J. J., and K. R. Porter. 1976. Stereo high voltage electron microscopy of whole cells of the human diploid cell line WI-38. *Am. J. Anat.* 147:303–324.
32. Wolosewick, J. J., and K. R. Porter. 1979. Microtrabecular lattice of the cytoplasmic ground substance: Artifact or reality? *J. Cell Biol.* 82:114–139.